NASA TT F-10,729

EXPERIMENTAL STUDY OF SINGLE-DEGREE OF FREEDOM FLUTTER IN TRANSONIC FLOW

H.Loiseau

Translation of "Étude expérimentale des flottements à un degré de liberté en écoulement transsonique". France, Office National d'Études et de Recherches Aérospatiales. Chatillon-sous-Bagneux, TN-95, 1966.

NATIONAL AERONAUTICS AND SPACE ADMINISTRATION
WASHINGTON FEBRUARY 1967

TABLE OF CONTENTS

		Page
I.	INTRODUCTION	1
II.	GENERAL PRINCIPLES	2
III.	MEASUREMENTS OF NONSTATIONARY COEFFICIENTS OF THE AILERON IN TRANSONIC REGIME	9
	III.1 Basic Principle	9
	III.2 Two-Dimensional Tests	10
	III.3 Three-Dimensional Tests	16
IV.	INFLUENCE OF THE REYNOLDS NUMBER	18
V.	SCHLIEREN TESTS IN TWO-DIMENSIONAL FLOW	21
	V.1 Installation	21
	V.2 Wing with Aileron of 0.3 Relative Chord	23
	V.2.1 Laminar Flow	23
	V.2.2 Turbulent Flow	31
	V.3 Wing with Aileron of 0.5 Relative Chord	34
	V.4 Flutter Domains	41
VI.	CONCLUSIONS	41

EXPERIMENTAL STUDY OF SINGLE-DEGREE OF FREEDOM FLUTTER IN TRANSONIC FLOW

/1**

H.Loiseau

Studies on a wing with aileron are reported; three types of instability are shown to exist. These occur when: A) the shock wave is ahead of the hinge; B) the shock wave is on the aileron; C) the shock wave is attached to the aileron trailing edge. These three types are encountered in different Mach number ranges. The effects of Reynolds number and aspect ratio are studied for each type. The work has not been extended to thick wings or to high-frequency parameters.

I. INTRODUCTION

Previous tests have demonstrated the rapid variation in the hinge moment coefficients of an aileron beyond the critical Mach number of the profile. The shock waves might generate instabilities as they are frequently encountered in wind-tunnel tests or in free flight with mockups or even in the full-scale aircraft, consisting of - on the one hand - flutter in one degree of freedom (for example, coupling between wing or aileron and the shock wave) and - on the other hand - of divergence.

The predominant influence of the Reynolds number has been proved in systematic tests in which either the generating pressure or the extent or position of the roughness strips intended for inducing turbulence were variable. Curves for the hinge moment coefficients of the aileron, in the transonic range, have been discussed in various papers published after tests made by the ONERA*. In addition, a large number of publications on this subject have appeared in other countries (Ref.1, 2, 3).

So as to obtain a better understanding of these phenomena, still other experiments were made with the schlieren technique, showing the mechanism of flutter in one degree of freedom, for a few special cases. This particular study, although quite incomplete, may assist in developing theories with allowance for the presence of shock waves on the profile, in the transonic regime. In fact, it is known that at present no possibilities for mathematical prediction in this relatively little known domain are in existence.

---

* ONERA = Office National d'Études et Recherches Aérospatiales (National Aerospace Research and Development Administration, France).

** Numbers given in the margin indicate pagination in the original foreign text.

II. GENERAL PRINCIPLES

It seems advisable to first give a succinct review of this problem, based on various recently published papers and on our own experiments; we will discuss exclusively flutter phenomena predicted by the theory of velocity potential flow and flutter phenomena due to interactions between boundary layer and shock wave. Instabilities such as buffeting, the flutter of detachment, whose nature is quite different will not be considered here.

Between the two critical Mach numbers of the profile, a domain which by definition constitutes the transonic regime, there exist three types of instabilities determined experimentally on wing models with ailerons and having widely differing mechanisms (Ref.3): /2

a) The recompression shock wave is ahead of the aileron hinge: instability A (Fig.1a).
b) The shock wave is attached to the aileron: instability B (Fig.1b).
c) The aileron is entirely supersonic: instability C (Fig.1c).

The instability A apparently is restricted to thick profiles and does not appear spontaneously. The motion must be damped by creating a relatively large perturbation, for example by giving the aileron a strong initial incidence and by extending it.

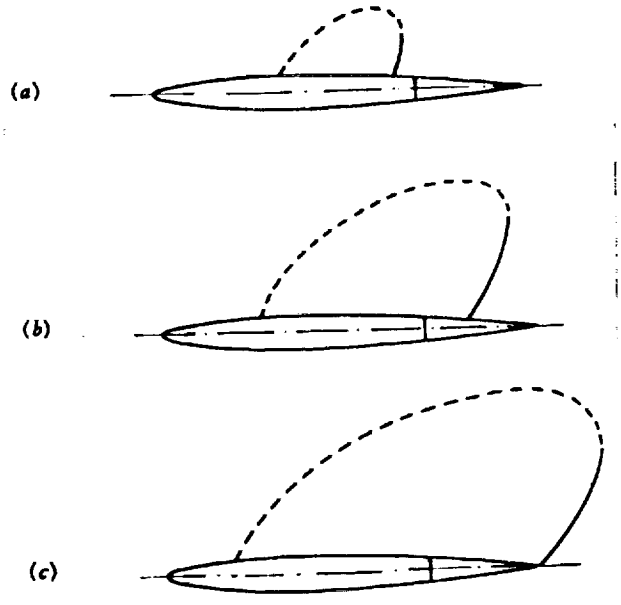

Fig.1
Instability domain A; Instability domain B;
Beginning of instability domain C.

On a profile on which this flutter exists, the damping will become positive again as soon as the shock wave reaches the hinge of the control surface.

We have never encountered this type of instability reported by Lambourne (Ref.3), neither in a wind tunnel nor in free air, probably because of the fact that all of our experiments were made on profiles of a relative thickness below 8%.

Conversely, from the very first experiments of measuring the hinge moments in the transonic regime, the instability B was systematically obtained. This instability appears spontaneously for a well-defined Mach value in a very narrow Mach variation range.

In this case, the shock wave is a certain distance aft of the aileron hinge. The phenomenon is highly explosive. /3

The second type of fluttering was mentioned by various authors (Ref.1 - 3) but has been encountered only at rare instances. The same investigators reported irregular vibrations of the aileron which is in opposition to our own observations (see Chapt.VI, Sect.2) if the influence of the nature of the boundary layer is disregarded, a point to be discussed in more detail later in the text (the Reynolds number has a considerable influence on the explosivity of the instability which is extremely high in laminar flow with sinusoidal aileron oscillations; the instability disappears almost completely when the turbulent boundary layer is sufficiently thick; in this case, only a few rather disordered vibrations of low amplitude are observed).

The end of the flutter is just as abrupt as the onset.

The instability C appears as soon as the Mach number at infinity upstream is slightly above 1. We have observed very smooth onsets of flutter and a stabilization of variable amplitude with the Mach number.

This latter type of flutter is predicted by the theory of velocity potential flow. According to our own observations, the flutter is somewhat influenced by the Reynolds number; in a laminar flow it does not always appear spontaneously. This is rather paradoxical since the theory, predicting this flutter, disregards the phenomena connected with viscosity. At other occasions (tests on delta wings in supersonic regime) we found that the onset of turbulence tended to approach the experimental results to the theoretical results, irrespective of the existing Mach number.

Our tests also showed that the instability B is highly sensitive to the wing aspect ratio. It disappears rapidly in the three-dimensional regime as soon as the wing aspect ratio diminishes.

Conversely, the (potential) flutter of type C exists even on delta wings with ailerons and even if these are located close to the wing tips.

It is probable that, as soon as the reduced frequency rises, certain of these flutter phenomena will disappear. Unfortunately, we have no valid experiments at high frequency at our disposition. It is rather difficult to produce mockups with one degree of aileron freedom, without risking deformation of the aileron and without coupling with the degrees of freedom of wing twist. On the other hand, in wind tunnels, the turbulence spectra admit of high frequencies,

and resonance phenomena of the air stream frequently generate sinusoidal vibrations of the models, having nothing to do with flutter.

The reduced frequency to be considered for a given aileron must logically be referred to the chord of the aileron itself rather than to the wing chord, /4 in supersonic flow. In fact, in this case the fixed portion ahead of the aileron theoretically does not intervene at all. (In practice, this plays a role only over the intermediary of the boundary layer which it produces along the aileron.) It follows from this that the reduced frequencies of our tests generally are very small. To diminish the risk of deformation and coupling and to permit two-dimensional tests, one solution would consist in using a relatively narrow and very high test section, with the length of the wing being equal to the width of the test section. This reduces to designing a special wind tunnel which, in turn, constitutes a difficult and tedious solution.

The theory predicts the onset of flutter of type C at Mach 1.0, which is more or less verified experimentally, with a slight lag in Mach number. The end of flutter (theoretically at $M = \sqrt{2}$) has not yet been verified because of the fact that no continuous wind tunnel between Mach 1.3 and 1.5 is available.

The effects of the angle of attack have not yet been studied and we have no information on this subject except for the data given elsewhere (Ref.3).

Another difficulty lies in the appearance of divergence close to Mach 1.0. The end of the nonstationary instability (B) precedes the onset of divergence by very little. Close to the velocity of sound, the phenomena are not linear and the significance of the Reynolds number is considerable here; when Re increases, the extent and the intensity of the divergence increase also.

At low frequencies, i.e., for low structural flexural rigidity of the aileron, the latter will deflect upward or downward until it strikes the stops. In that case, no measurement at all is possible.

On increasing the flexural rigidity, and thus the frequencies, the aileron will deflect positively or negatively, with the angle of deflection decreasing with increasing stiffness, which is characteristic for the nonlinearity of aerodynamic rigidities (if they were linear, as the structural rigidity, the sum of both would have an indifferent amplitude sign and no equilibrium amplitude different from zero could exist).

If the aileron is made to oscillate about the nose-up equilibrium position, the frequency response will not be sinusoidal. In this domain near Mach 1.1 it is impossible to define values for the nonstationary hinge moment coefficients in phase with the displacement or the velocity, without correlating them with the mean angles of attack of the wing and of the aileron and with the instantaneous angles of attack, which considerably complicates the problem.

a) Tests for Defining the Mechanism of Instabilities A and B /5

The instability C is predicted by the theory of velocity potential flow. The two other, much more complex, instabilities are not readily accessible to

calculation.

Using a rigidly fixed two-dimensional wing model without aileron, Kawamura and Karashima (Ref.1) demonstrated experimentally that the system of shock waves is able to oscillate, at a certain frequency depending on the dimensions of the profile, in the case of laminar flow. This oscillation is obtained, for example, by creating a perturbation downstream of the wing (abrupt variation in pressure) and is then damped like a system of one degree of freedom. The oscillation exists only in a narrow Mach number range (about M = 0.9 for the tested profile of 10% relative thickness). The phenomenon disappears in turbulent flow.

The oscillation frequencies were 2500 cps for a profile of 24 mm chord and 1430 cps for a profile of 48 mm chord. On extrapolating to the dimensions of wings tested by us (l = 200 mm), the corresponding frequency will become 300 cps, meaning that ω_R with respect to the wing will become 0.6 to 300 m/sec. Such an extrapolation is risky and the scale effect definitely will not be linear; there is no doubt that the Reynolds number will intervene here by modifying the frequency; however, the value of 300 cps is not excessively wrong. Flutter of type B, observed by us, showed frequencies between 30 and 150 cps. Thus, if the flexural rigidity of the aileron is increased further, the tendency to flutter will still be present. The fact that instability is rarely encountered in the full-scale aircraft is due more to the influence of the aspect ratio and of the Reynolds number than to the value of the reduced frequency.

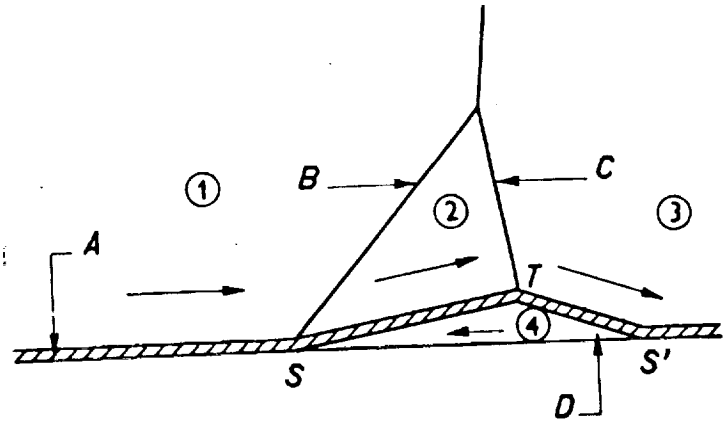

Fig.2
A - Laminar boundary layer; B - Recompression shock upstream; C - Recompression shock downstream; D - Zone of flow separation.

The flow can be schematized as shown in Fig.2 (Ref.1, 4).

This scheme corresponds to a flow with laminar boundary layer, for example, midway between the lower critical Mach number of the profile and 1. The zones /6 (1) and (2) are supersonic while the zone (3) is subsonic. If p_1, p_2, and p_3 represent the pressures in the zones (1), (2), and (3), then p_3 will be larger than p_2 and the latter, in turn, will be larger than p_1. Let us recall that the laminar boundary layer is characterized by a considerable thickness of its subsonic portion. The upwash from (3) toward (2) thus is intense, producing flow separation and creation of the zone (4). At fixed Mach number and without external perturbation, equilibrium will be established. The velocities are as

indicated by the arrows. A perturbation in the zone (3) will propagate into the zone (2) passing through the zone (4). If the profile is fixed, the perturbation can come only from a source exterior to the model. No matter what type of source this might be, let us assume that it causes the rear shock wave to shift toward the front. The velocity increases across this shock, resulting in a pressure rise in the zone (3). This pressure increase is transmitted to the zone (4) and then to the zone (2), reaching the rear shock wave on the upstream end. The increase in pressure on this side of the shock wave stops its motion toward the front. This results in a reduction of the excess pressure in the zone (3), and so on. Practical experience shows that the shock wave oscillates a certain number of times. The quarter-period of oscillation can be calculated in two different manners (Ref.1):

a) The perturbation is transmitted by the separation zone toward the separation point S which advances, entraining the bow wave. This results in a pressure rise aft of this shock wave, which reaches the downstream shock wave after a certain time. Taking into consideration the fluid and sonic velocities in the zones (4) and (2) and knowing the length in direction of the wind of the separated zone between the bases of the shock waves, it is easy to calculate the total time required by the perturbation effect to travel from the downstream to the upstream end of the rear shock wave.

b) It is assumed that the dimensions of the separated zone oscillate horizontally or that the angle TSS' varies periodically. Consequently, the domain (2) oscillates in accordance with the motion of the zone (4). Allowance is made for the time required for the separated region to fill again. This time is calculated on the basis of the fluid velocity in the zone (4) and the dimensions of this domain. An enlargement of the flow separation zone will lead to a forward shift of the bow wave and thus to a variation in pressure which is then transmitted toward the rear shock wave.

An overpressure aft of the bow wave [in the zone (3)] due to a forward motion of this shock wave will increase the flow in the separation zone, which produces a frontward shift of the separation point S. The phase shift in time /7 between the pressure rise in the zone (3) and the pressure rise upstream of the rear shock is equal to the time of filling of the zone (4), increased by the propagation time in the zone (2).

Both methods lead to highly acceptable orders of magnitude for the oscillation frequency. However, the second method, which takes into account the masses and volumes of the fluids in motion, yields a value closer to the experimental results than the first method which considers only the propagation times.

These oscillations are produced only in a narrow Mach range, a fact still inadequately explained.

b) Theories Considering the Profile Shape

Starting from conventional hypotheses, Coupry (Ref.5), taking into consideration the thickness and shape of the profile, obtained theoretical values for the hinge moment coefficients, in phase with the displacement or the velocity

and in excellent agreement with experimental results, for Mach numbers slightly above 1, and theoretically also proved the existence of control-surface buzz.

In this theory, the stationary solution of the velocity potential is assumed as known, and then is replaced by a simpler schematic solution such that equations relatively easy to solve are obtained. The experimental values of the hinge moments (n_d' and n_d''') are in satisfactory agreement with the theoretical results directly above Mach 1.0.

It is certain that, for aileron coefficients above Mach 1.0, it is always of advantage to consider the local Mach number which generally is very much higher than 1.0.

We should mention experiments made by Nakamura and Tanabe (Ref.2) which have numerous points of similarity with the experiments described below. However, in these experiments, main emphasis was on studying the initiation of flutter predicted by the theory of the velocity potential flow.

Flutter of the region A was not encountered despite the fact that the profile of the mockup was large (10%). Flutter of type B appeared in a nonsinusoidal form mixed with the divergence. The boundary layer was artificially rendered turbulent.

c) Examples of Instability Encountered in Free Flight with Mockup or Aircraft in the Wind Tunnel

An example of buzz was reported by Coupry (Ref.5), obtained during transonic flight tests of an aircraft prototype with sweptback wings. /8

It seems that cases of buzz on full-scale aircraft are relatively rare. Conversely, during various tests on models, numerous such examples were encountered.

Fig.3 Aileron Flutter in One Degree of Freedom, for a Straight Wing of Aspect Ratio 2.2.
Upper band: aileron vibrations } accelero-
Lower band: wing vibrations } meters.

On mockups launched in free fall, equipped with straight wings of 0.225 m span and 0.205 m chord (i.e., an aspect ratio of 2.2) and having an aileron extend over the entire length of the wing of 0.30 relative chord, aileron vibrations were observed at a Mach number close to 0.95 (Fig.3).

This flutter may be influenced slightly by couplings with the wing

(since, at subsonic speeds, a coupling flutter existed between the flexure of the wing and the rotation of the aileron, ranging from M = 0.73 to 0.86 for one of the models and from 0.60 to 0.80 for the other model; see Fig.4).

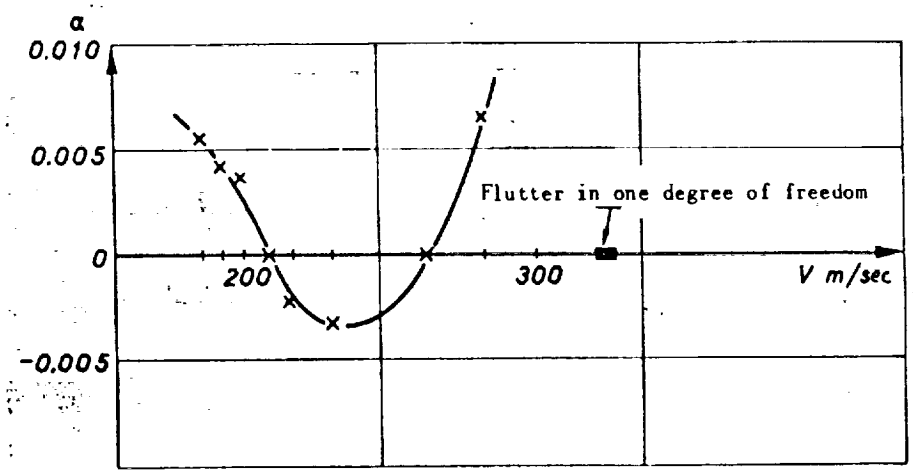

Fig.4

We should also mention a type of flutter that apparently is related with /9 the instability predicted by the theory of velocity potential flow, encountered on wind-tunnel models equipped with delta wings (in one case with a sweptforward trailing edge and in the other case with sweptback trailing edge). Data on the characteristic vibration modes without wind showed modes in which the vibrating portion is practically restricted to the zone located close to the trailing edge (Fig.5), exactly as though the wing had been equipped with an aileron whose hinge is shown as a broken line.

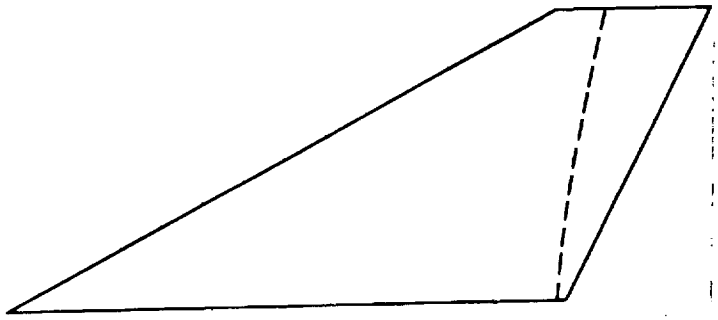

Fig.5

The vibrations observed in flight are difficult to attribute to a coupling between two or more modes. Most likely, single-degree of freedom flutter is involved here (Figs.6 and 7).

Another report (Ref.6) gives results of measurements of aileron hinge /10 moments in free flight, on dropped models (straight wing of 2.25 aspect ratio, relative profile thickness 9% at 40% of the chord, with an aileron of 0.25 relative chord over the entire wing span). The transition was natural, but the

Reynolds number was sufficient for initiating it. The hinge moment coefficients, in phase with the velocity, cancel toward Mach 0.94. Slight aileron vibrations of a rather disordered but nonsinusoidal type were observed. Close to Mach 1.0, the damping assumes high positive values and then decays slightly above Mach 1.0. The supersonic flutter is not excessively explosive and the vibration is sinusoidal.

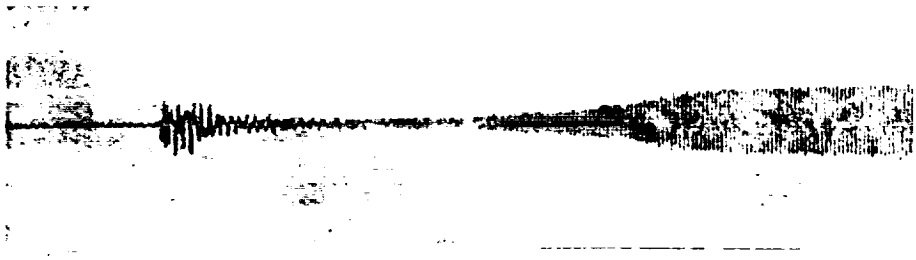

Fig.6 Start of Flutter Observed on a Delta Wing with Sweptforward Trailing Edge, Preceded by an Impulse Produced by an Explosive Charge.

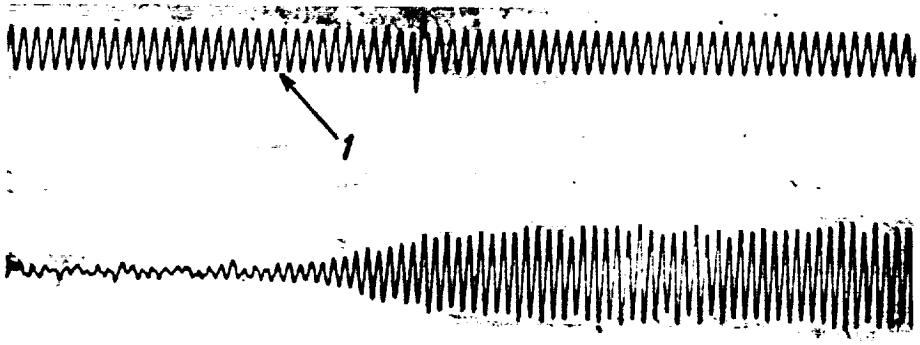

Fig.7 Start of Flutter on a Wing of the Type Shown in Fig.5. Upper curve: time base at 200 cps.

Finally, in systematic measurements on the hinge moment coefficients in a wind tunnel, in two-dimensional flow, the main difficulties encountered in the transonic regime are connected with the systematic appearance of the instability B, which is extremely abrupt in a laminar flow. The following Chapter will give an accurate account of the experiments made. The experimental values are omitted here, except for some that have not yet been published.

III. MEASUREMENT OF NONSTATIONARY COEFFICIENTS OF AN AILERON IN TRANSONIC FLOW

II.1 Basic Principles

No matter what type of model is considered, the basic principle of measurement remains the same. The ailerons are hinged to the fixed surfaces by crossed flexible fittings. The horizontal attachment strip extends over the entire

length of the aileron such that no circulation can take place between the suction side and pressure side at the level of the hinge. Study of the influence of the reduced frequency is made possible by varying the rigidity of the individual strips.

The moment of aerodynamic forces relative to the hinge reads

$$\mathfrak{M} = -\pi \frac{\rho V^2}{2} S \frac{l}{2} n_d \Theta$$

where

M = hinge moment
ρ = volume mass of air
V = wind velocity
$\frac{l}{2}$ = reference length (1/2 wing chord)
n_d = dimensionless hinge moment coefficient.

$$n_d = n'_d + j n''_d \qquad n''_d = \omega_R n'''_d$$ /11

where

$\omega_R = \omega \frac{l}{2} \frac{1}{V}$ = reduced frequency

ω = pulsation
n'_d = real coefficient or in phase with the displacement
n'''_d = imaginary coefficient, or in phase with the velocity.

The relative chord of the aileron is denoted by τ.

If c is the aileron chord, then $\tau = \frac{c}{l}$.

The real and imaginary coefficients, referring to the dimensions of the ailerons, are n'_d/τ^2 and n'''_d/τ^3, respectively.

The values of the real coefficients result from measuring the aileron frequency variations with and without wind.

The imaginary values are obtained either by measuring the excitation forces required for making the aileron oscillate in its phase resonance at practically the same amplitude rate with and without wind, or else by measuring the dampings with and without wind.

III.2 Two-Dimensional Tests

III.2.1 Test with a Wing Oscillating about the Leading Edge or an Aileron of Relative Chord of Unity (Fig.8)

The relative thickness of the profile is 6%.

The transition is generated at the maximum cross section (40% of the chord)

and at the leading edge (see Chapt.IV on the influence of the Reynolds number).

Figures 9 and 10 give the experimental values for the coefficients n'_d and n'''_d, defined previously between Mach numbers of 0.4 and 1.2, for various values of the reduced frequency. These values are entered above the test points in the

/12

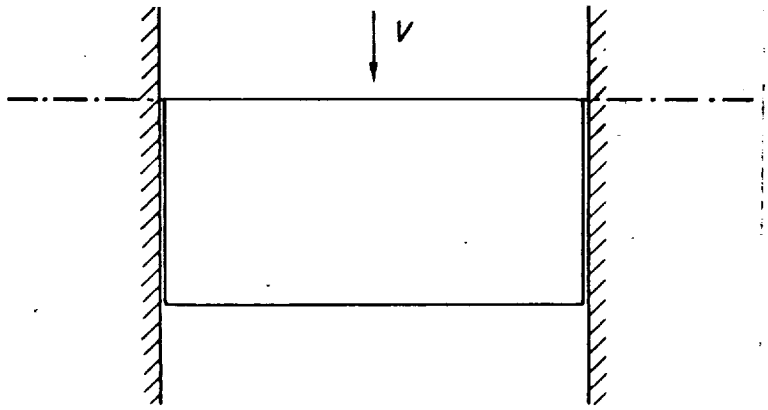

Fig.8

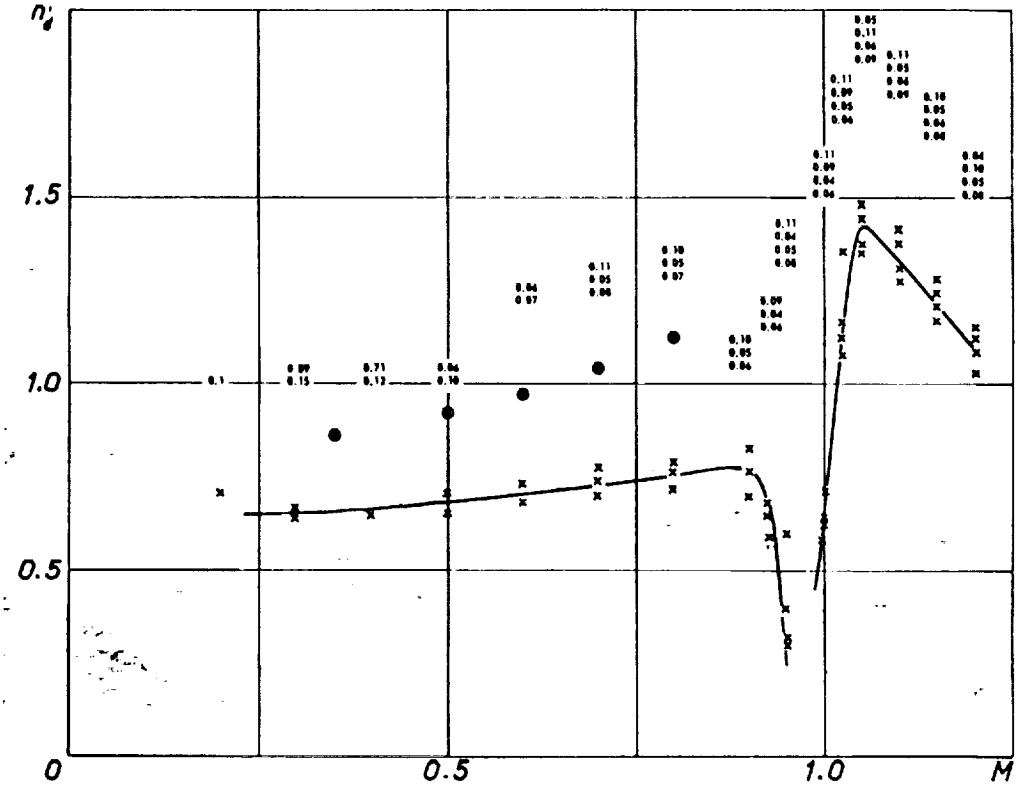

Fig.9 $\tau = 1.0 - n'_d$ as a Function of the Mach Number; Two-Dimensional Wing Oscillating about the Leading Edge with Induced Transition. ⊙: Theory (Ref.8) for $\omega_R \approx 0.1$.

order of the coefficients. It is immediately obvious that the variations in the coefficients as a function of the reduced frequencies are too weak in the range of variation of the latter for deriving any law of evolution. The observed differences can be attributed entirely to scattering of the test points. Consequently, mean evolution curves of n_d' and n_d''' were plotted as a function of M, for a mean reduced frequency value of 0.1.

Here, n_d' tends to become negative in the neighborhood of Mach 1, at low amplitudes (considerable nonlinearity at Mach 1.0).

The coefficient n_d''' has a poorly defined maximum near 0.93. No damping /13 of the flutter below 1.0 can be distinguished. The flutter (of type C) is only moderately explosive. The negative damping points are obtained by successively blocking and freeing the wing. The given values are corrected for the influence of the boundary layer at the wall (the wing length is diminished in accordance with the velocity profile in direction of the span).

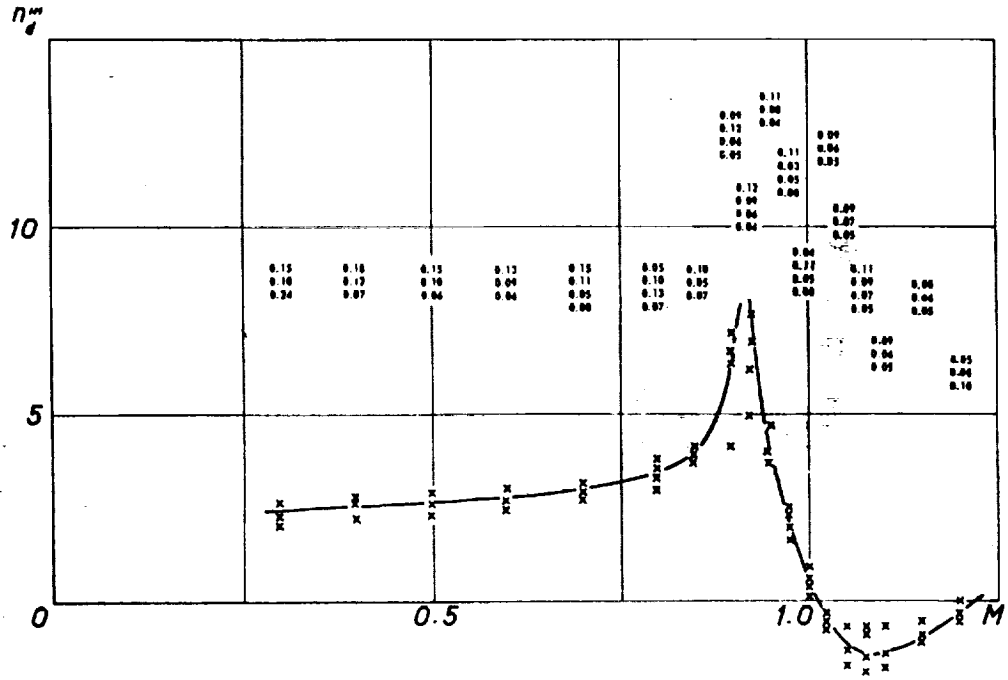

Fig.10 Two-Dimensional Wing Oscillating about the Leading Edge; Induced Transition; n_d''' as a Function of the Mach Number.

III.2.2 Wing Equipped with an Aileron of 0.5 Relative Chord, over the Entire Length of the Wing (Fig.11)

The coefficients were measured only in the subsonic regime. The values n_d'/τ^2 and n_d'''/τ^3 are plotted in Figs.12 and 13, with τ being the dimensionless value of the aileron chord, which reduces to giving the hinge moment coefficients as a function of the aileron dimensions without consideration of whatever might be in front of this point.

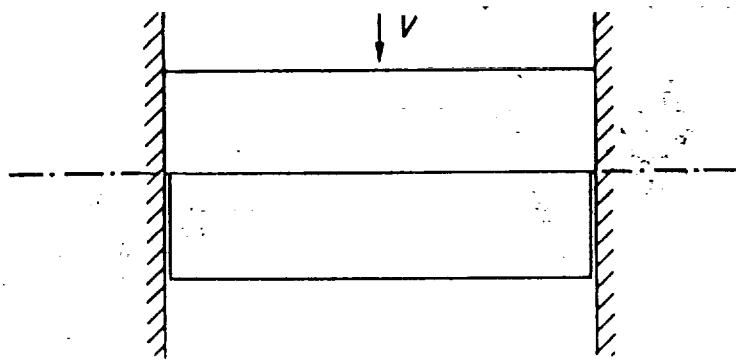

Fig.11

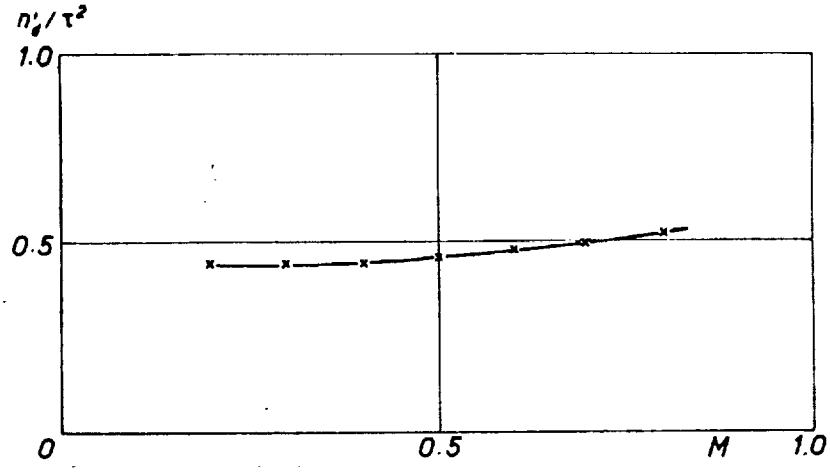

Fig.12 Two-Dimensional Wing with Aileron of 0.5 Relative Chord; n'_d/τ^2 as a Function of the Mach Number.

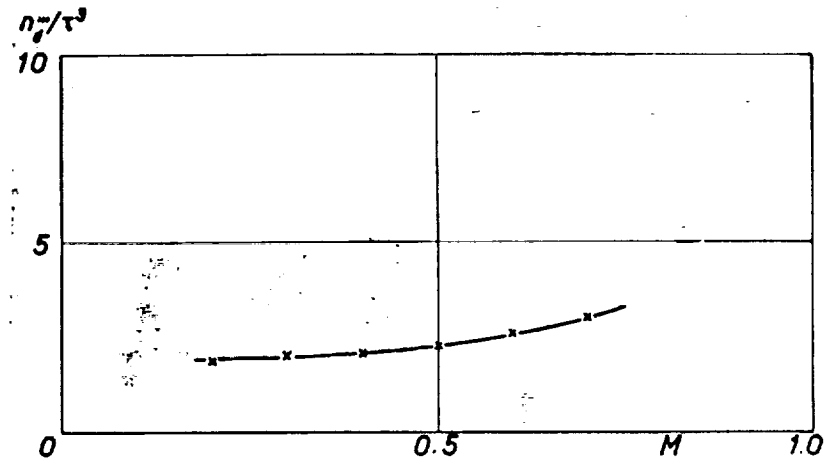

Fig.13 Two-Dimensional Wing with Aileron of 0.5 Relative Chord; n'''_d/τ^3 as a Function of the Mach Number.

The reduced frequency is equal to 0.1, a value which again is referred to the aileron chord.

A flutter of type B, sensitive to the Reynolds number, was observed (see Chapt.IV), together with a weak flutter of type C.

III.2.3 Two-Dimensional Wing Equipped with an Aileron of 0.3 Relative Chord, over the Entire Wing Length /15

The values plotted in Figs.14 and 15 correspond to a reduced frequency of 0.1, as in the previously mentioned tests (always referring to the aileron chord).

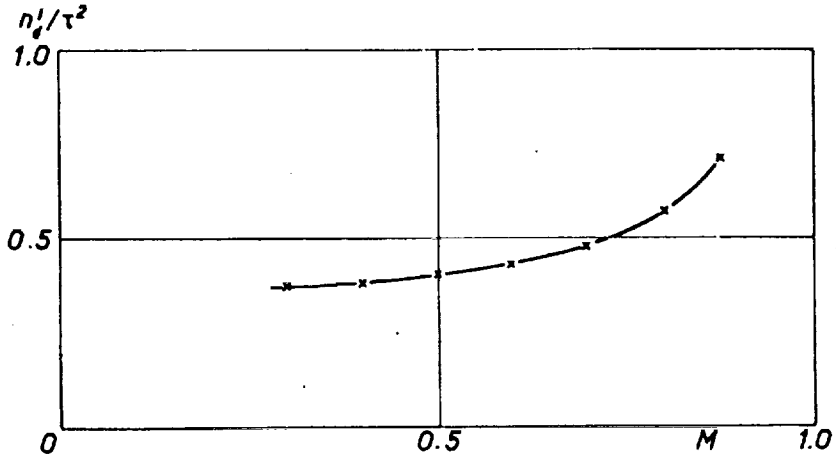

Fig.14 Two-Dimensional Wing with Aileron of 0.3 Relative Chord; n'_d/τ^2 as a Function of the Mach Number.

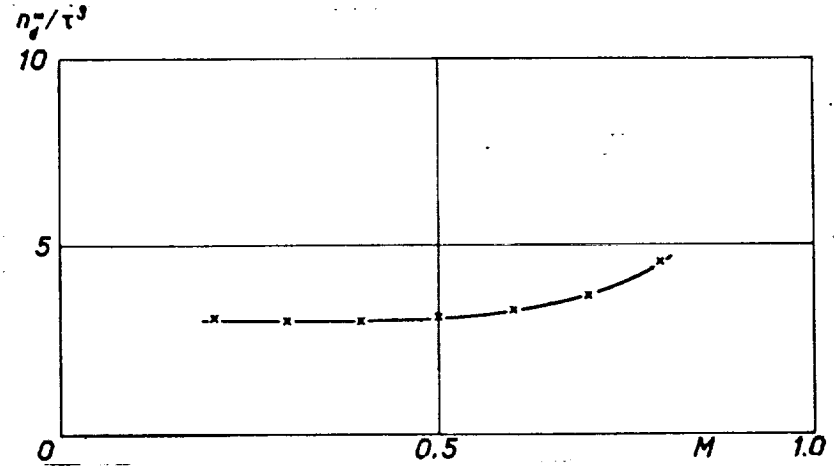

Fig.15 Two-Dimensional Wing with Aileron of $\tau = 0.3$ Relative Chord; n'''_d/τ^3 as a Function of the Mach Number.

The conclusions are the same as for the aileron of 0.5 relative chord: flutter of type B sensitive to the conditions of generation of transition, flutter of type C.

Note: /16

The real coefficient referred to the aileron diminishes slightly with decreasing relative chord (Fig.16). The imaginary coefficient increases under the same conditions (Fig.17).

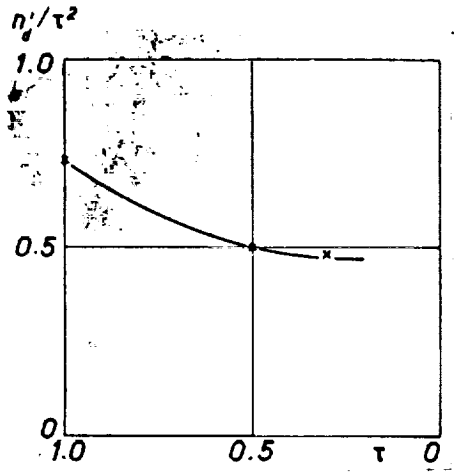

Fig.16 Real Hinge Moment Coefficient, Referred to the Aileron, as a Function of the Relative Chord at M = 0.7.

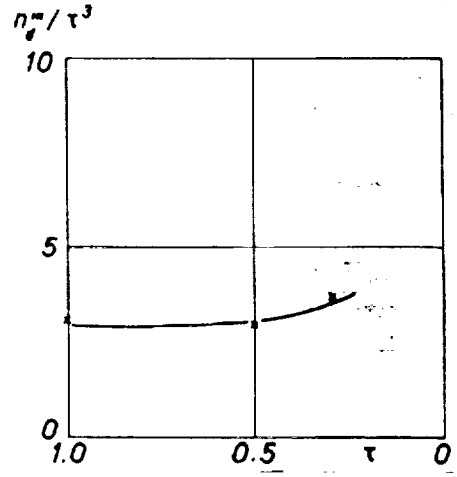

Fig.17 Imaginary Coefficient Referred to the Aileron, as a Function of the Relative Chord at M = 0.7.

Figure 9 also shows the theoretical values of n'_d, extracted from another paper (Ref.8).

III.2.4 Three-Dimensional Tests in Two-Dimensional Flow (Fig.18)

The purpose of these tests was to obtain coefficients for ailerons of very small aspect ratio. The symmetric geometric arrangement of these ailerons permits obtaining the direct coefficients (n'_d and n'''_d) defined above as well as the coefficients of coupling between the two ailerons n'_c and n'''_c. The experimental values were then compared with the calculated values (Ref.13) in low supersonic flow. /17 The experimental and theoretical results are given in detail elsewhere (Ref.7). A study of the influence of transition was made at the occasion of these tests, and the resultant effects will be discussed in Chapter IV.

Above Mach 1.0, the damping of the symmetric vibration mode (both ailerons vibrating in phase as though they were a single unit of double aspect ratio) was practically zero. Conversely, the damping of the antisymmetric vibration mode - although very weak - was distinctly greater, a fact which demonstrates

the effect of the aspect ratio on the instability C. Nevertheless, we believe that this aspect ratio effect is exaggerated by the coupling between the two ailerons. The effects of the slot between the fixed surface and the ailerons seem rather significant. We also observed the instability B, influenced by the transition.

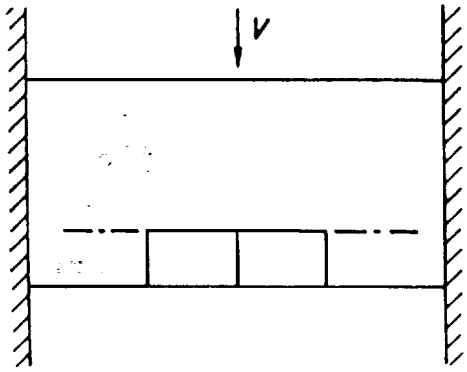

Fig.18

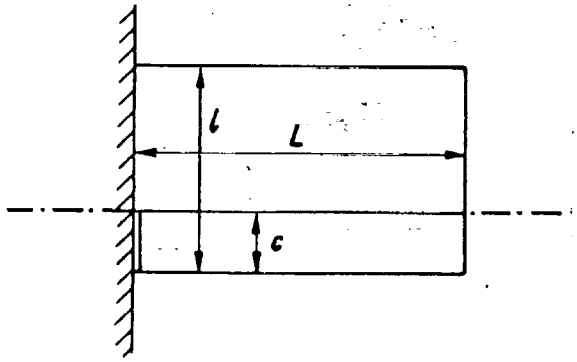

Fig.19

/18

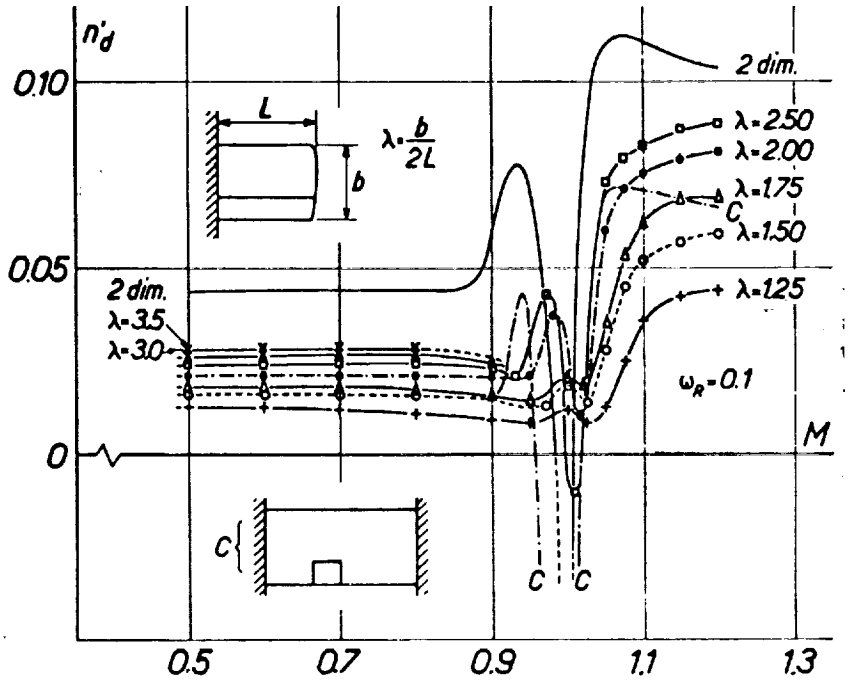

Fig.20

III.3 Three-Dimensional Tests on a Straight Wing of Variable Aspect Ratio (Fig.19); (Ref.7)

The results are shown in Figs.20 and 21 and correspond to an artificial generation of turbulence.

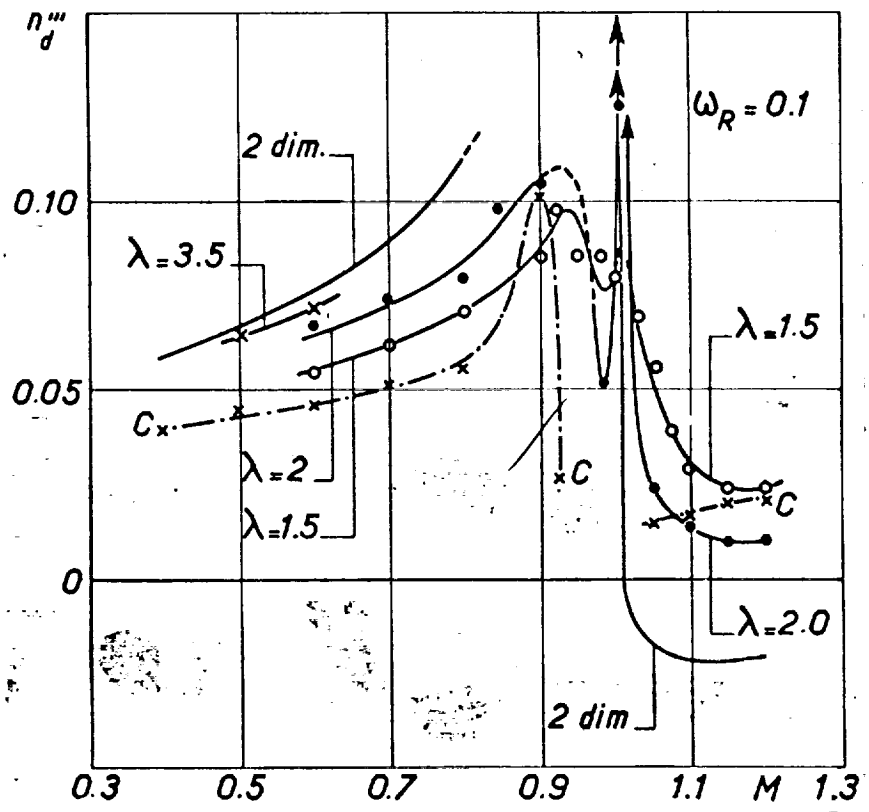

Fig.21

It is of interest to note the slope of the curves for the real coefficient, as a function of aspect ratio and Mach number. The divergence is especially pronounced in two-dimensional flow, even in the case of ailerons of low aspect ratio mounted to a two-dimensional wing. /19

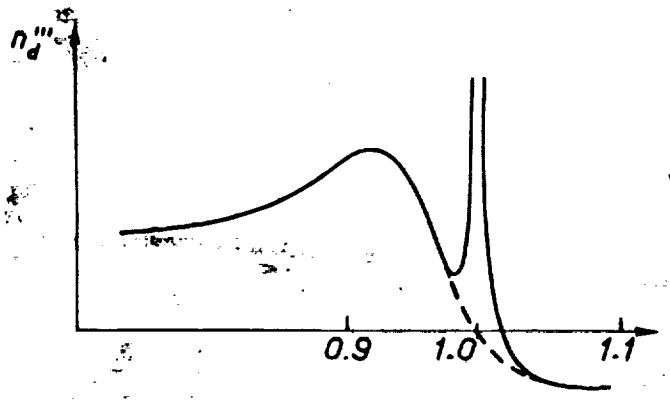

Fig.22

For an aspect ratio of $\lambda = \frac{2L}{l} = 2.5$, the coefficient n_d' is still negative near M = 1.0. For $\lambda = 2.0$, the coefficient is always positive.

A study of the curves n_d''' as a function of the Mach number, for aspect ratios of 2 and 1.5, shows a minimum close to M = 0.95. We do not believe that this minimum corresponds to the damped instability B. Rather, it seems to be due to abnormally high values close to Mach 1. Without

this discontinuity at Mach 1.0, the curve could be traced in a continuous manner from the subsonic to the supersonic regime (Fig.22).

IV. INFLUENCE OF THE REYNOLDS NUMBER

In all above-mentioned cases, an instability of the type B near Mach 0.92 to 0.94 was observed in natural transition, i.e., in a quasi-laminar flow. The flutter is highly explosive in the two-dimensional case, with its intensity decreasing with the aspect ratio.

The influence of the boundary layer was specifically studied for the case of ailerons of low aspect ratio (Fig.18). The rough transition strip was placed over the entire wing span on both suction and pressure sides, between 0.075 l and 0.125 l.

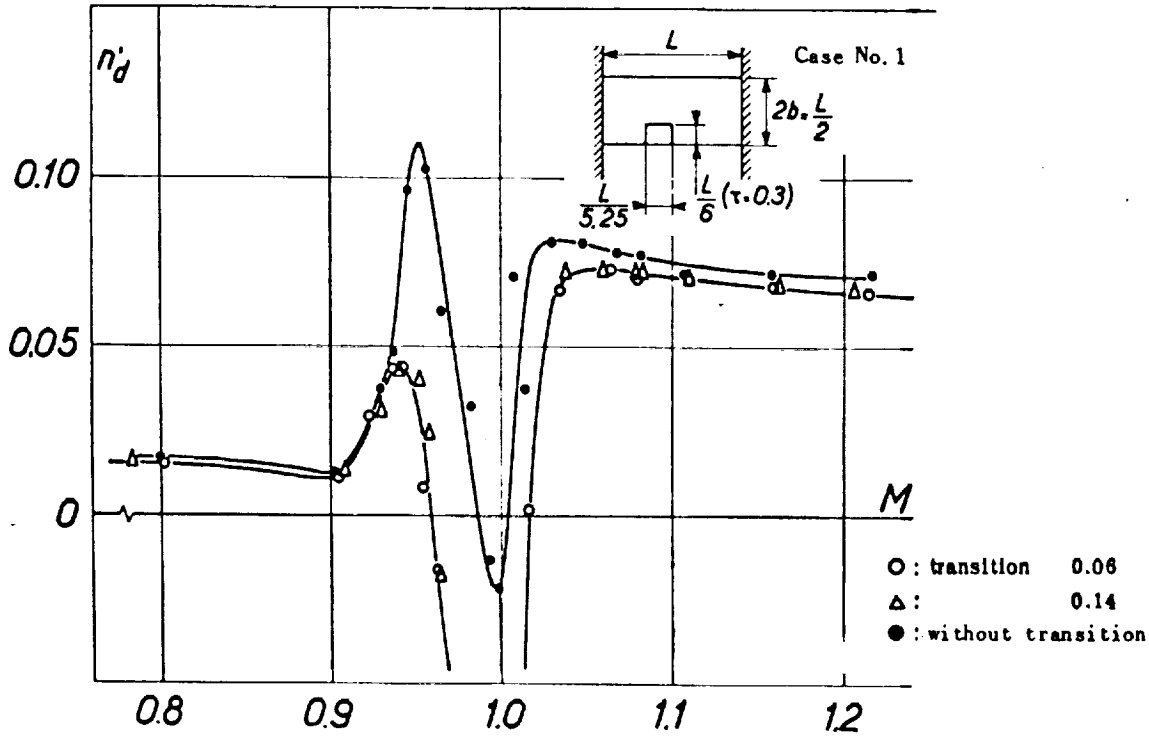

Fig.23

In induced transition, the divergence (Fig.23) is high in value and extent, depending on the Mach number. This observation was made in all other cases investigated, at least in a qualitative manner.

The tendency to flutter of type B diminishes (Fig.24). /20

In the subsonic range, for Mach values below the critical Mach number of

the profile, the real and imaginary coefficients are little influenced by the transition (Figs.24 and 25). It is also obvious that, for subsonic values of M, the coefficients n'_d and n'''_d correspond to the wing oscillating about the leading edge, indicating that the transition has little significance (Figs.26 and 27).

/21

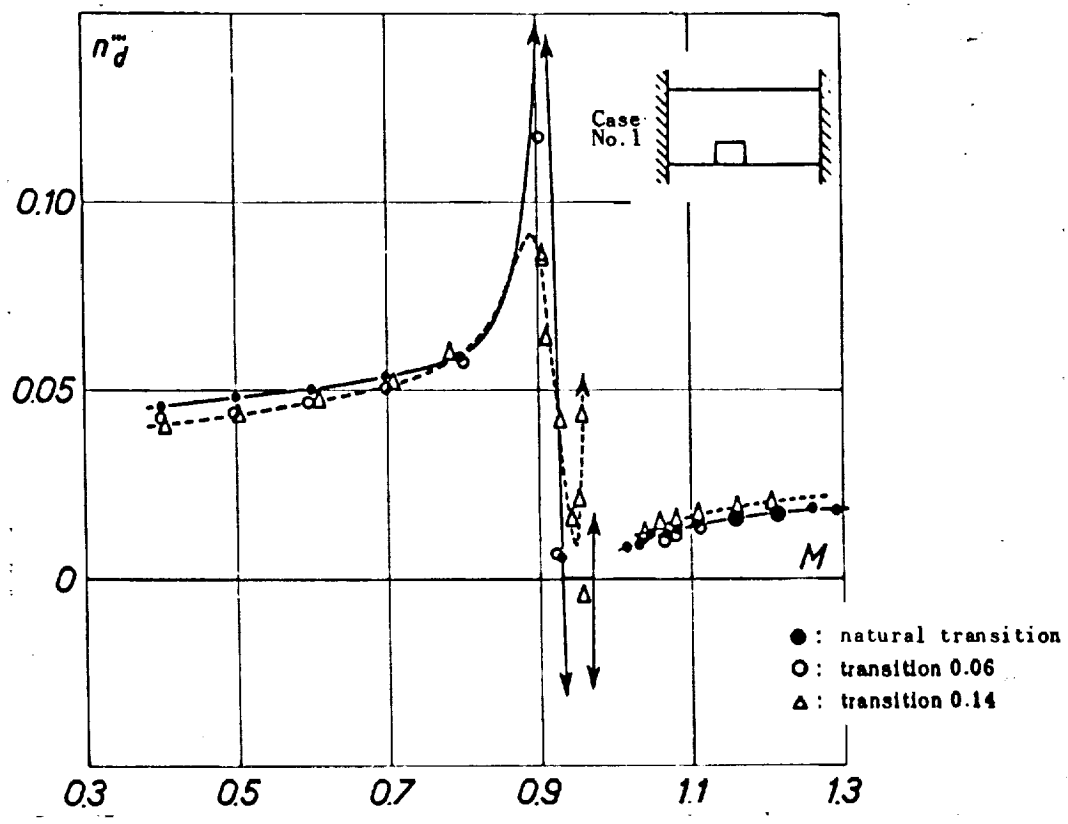

Fig.24

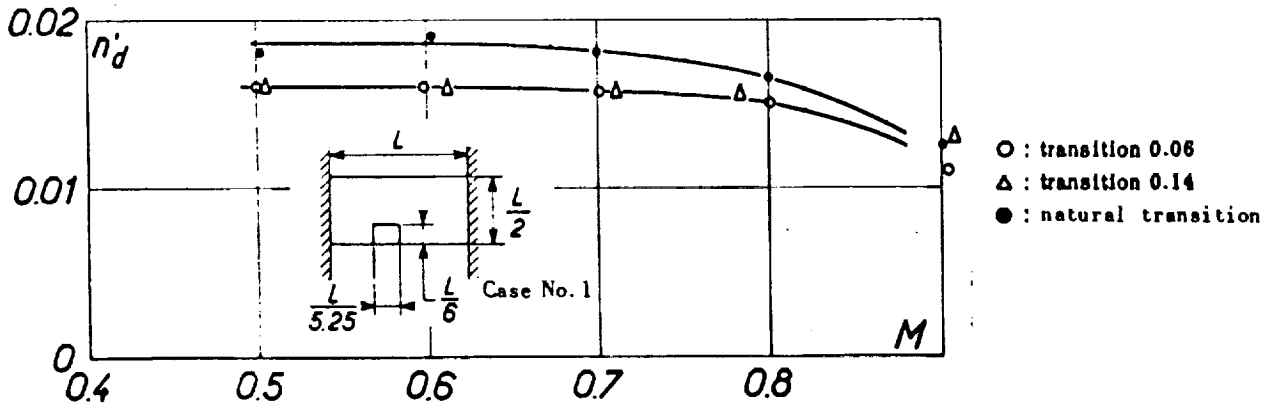

Fig.25

Figure 28 shows a damping curve as a function of the Mach number, corresponding to the case of a two-dimensional aileron of 0.3 relative chord. The

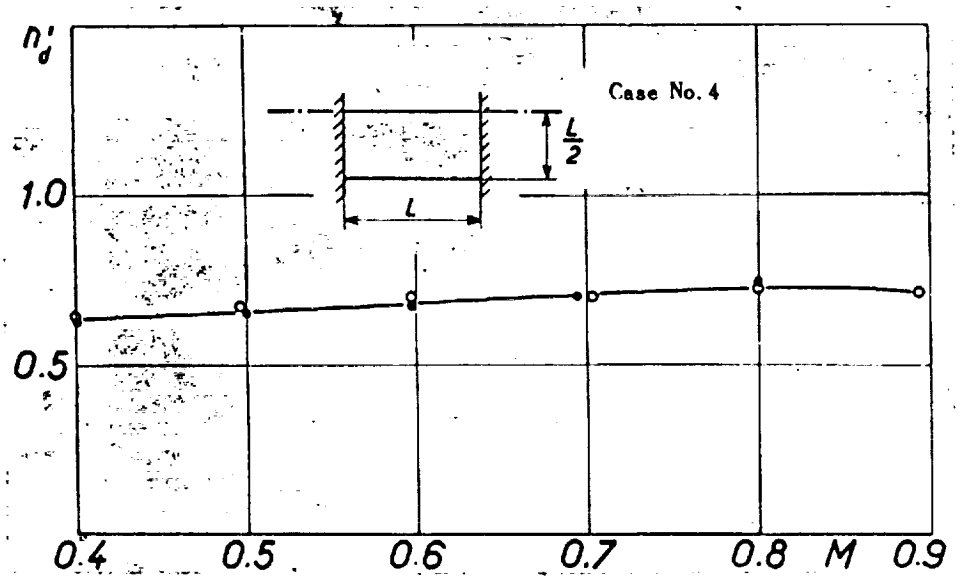
n_d'
Case No. 4
$\frac{L}{2}$
L
1.0
0.5
0.4
0.5
0.6
0.7
0.8
M
0.9
○ : transition 0.25
● : natural transition

Fig.26

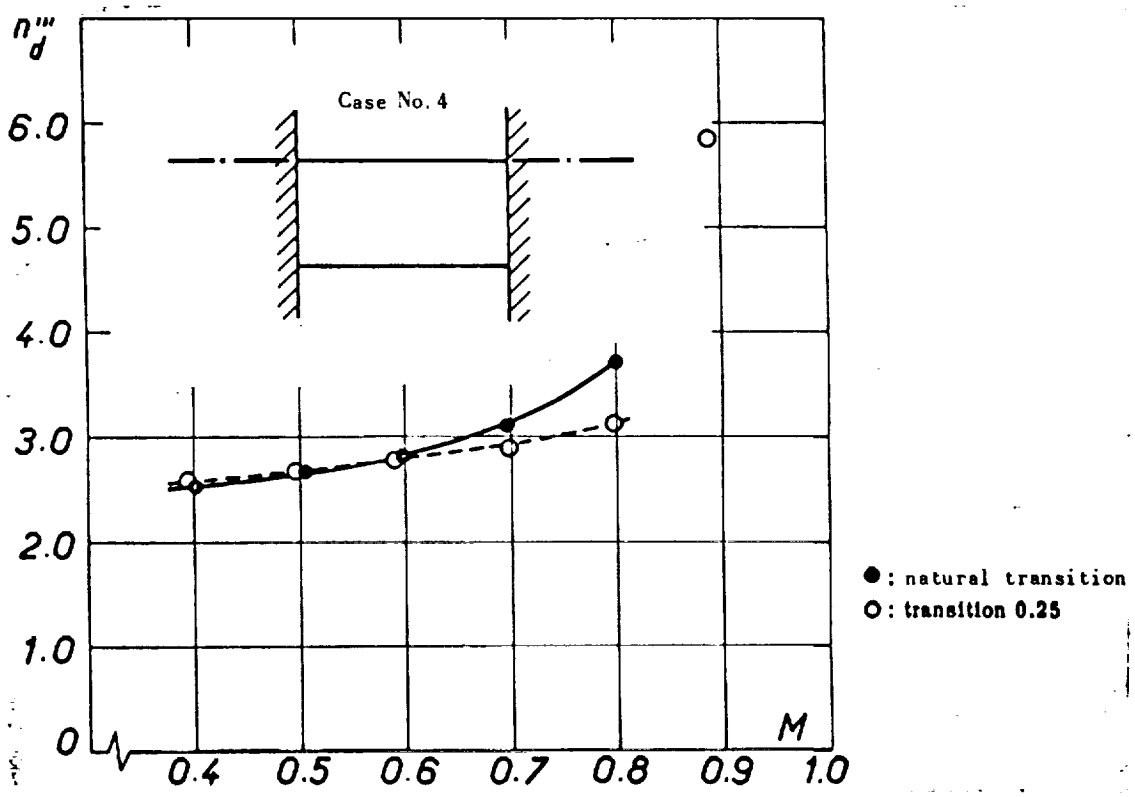
n_d'''
Case No. 4
6.0
5.0
4.0
3.0
2.0
1.0
0
0.4
0.5
0.6
0.7
0.8
0.9
1.0
M
● : natural transition
○ : transition 0.25

Fig.27

damping is negative close to 0.92 and then becomes high in positive value, simultaneous with the appearance of divergence between 0.95 and 1.025. If a rough transition strip is mounted to the main bulkhead and to the leading edge, the instability will disappear. If the transition at the leading edge is removed, the instability will not reappear. The transition (at equivalent roughness and width) is thus much more effective at the maximum cross section.

Recent tests on a mockup, simulating a slender delta wing placed at the center of the wind tunnel test section, yielded the same conclusion: Coherent results for the imaginary coefficients were obtained only if the transition was induced at the maximum cross section and at considerable roughness, each time that shock waves were present on the model. (These shock waves may be of the type normally observed in the transonic regime; however, they may also be due to parasite reflections on the walls of the test section or may originate at another part of the model. In laminar flow, the presence of a shock wave, no matter what its origin, may cause an instability. Flutter due to the interaction of the boundary layer with the shock wave is not restricted to the transonic region at a Mach number below 1.)

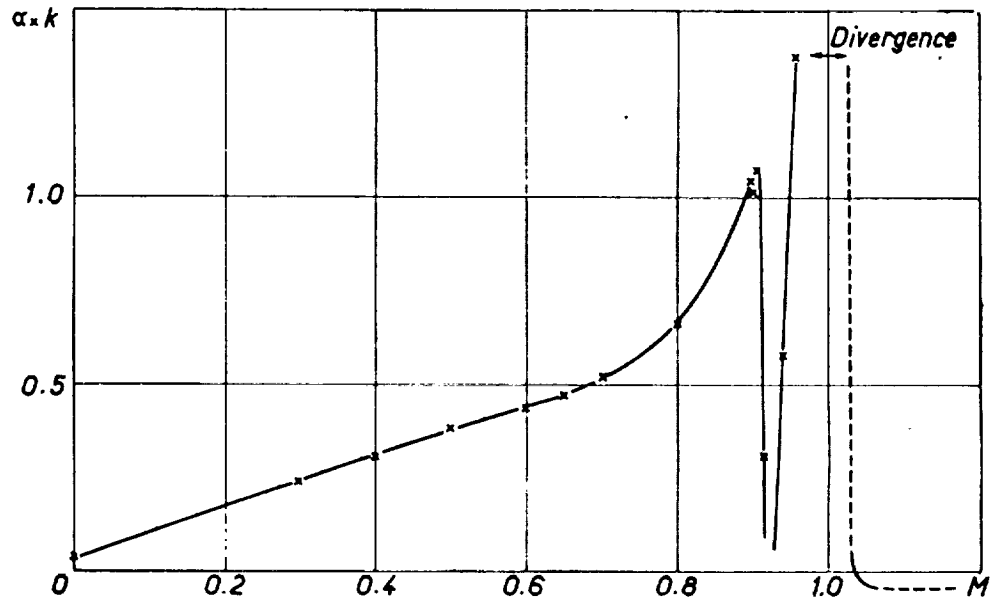

/23

Fig.28 Damping Curve - Aileron $\tau = 0.3$ - Transition at the Leading Edge.

V. SCHLIEREN TESTS IN TWO-DIMENSIONAL FLOW

V.1 Installation

The equipment is of the conventional type: A high-speed camera permits photographing the oscillations of the model and of the shock waves. Various exposure rates were selected, depending on the oscillation frequency and on whether orienting tests or definite tests were involved that later permitted

reconstitution of the motion at a slower rate with high accuracy, thus making an analysis of the mechanism of the phenomenon possible. The most rapid frame frequency was of the order of 2000 images per second. The exposure time was only a few seconds and we had considerable difficulty in filming the instability at the most opportune moment. In this process, the mode of operation was as follows:

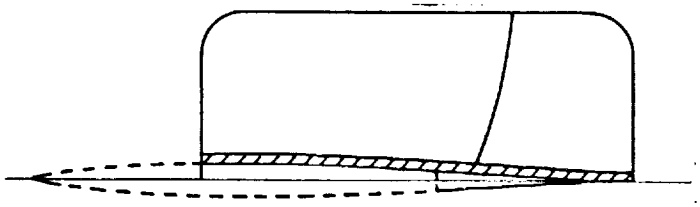

Fig.29

The schlieren picture was transmitted simultaneously to the camera and to a distant-viewing screen. In a preliminary test, the Mach number was increased slowly from the critical Mach number of the profile, and the position of the shock wave at the beginning of the instability was noted on the screen. In some cases, the model was damaged during the flutter. Nevertheless, since we used stops for limiting the oscillation amplitudes of the aileron, such accidents were an exception. After repair, if required, the experiment was resumed and the camera was started at the instant at which the shock wave reached the reference position. Since the Mach number was increased slowly so as not to modify the phenomena, the exposure time was shorter than the time of instability; therefore, observation of this instability had generally to be divided into three phases: onset of flutter, stabilized flutter, end of flutter. /24

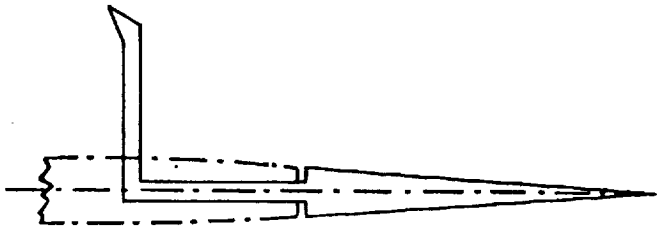

Fig.30

Since the profile was symmetric and the mean angle of attack of the wing and aileron was zero, the flow was symmetric with respect to the median surface of the wing. Subsequently, only one side was observed (Fig.29).

This arrangement had the advantage of permitting a rigid suspension of the model in the wind tunnel. The vibrations of the aileron were recorded over the intermediary of a velocity pickup. An electrodynamic exciter permitted harmonic excitation of the aileron. These apparatus were located entirely within the lower half-space. During data reduction, the schlieren pictures could be related with the corresponding recordings of aileron rotation.

In addition, some of the photographs show a rod integral with the aileron. The position of this rod, as a function of time, gives a highly accurate indication of the exact motion of the aileron during one cycle, which can then be compared with the motion of the shock wave so as to evaluate, in particular, the phase shift (Fig.30).

The dimensions of the model are the same as those of the mockup used in measuring the coefficients (Fig.11): length, 0.400 m; chord, 0.200 m; symmetric profile of 0.06 relative thickness at 40% of the chord.

Let us recall that the aileron was hinged to the wing by two crossed struts, one of the horizontal struts extending over the entire span. The trailing edge of the aileron had zero thickness (to within the manufacturing possibilities). The leading edge of the aileron is shown in Fig.31. /25

Fig.31

V.2 Wing with Aileron of 0.3 Relative Chord

V.2.1 Laminar Flow

During natural transition, the flow is practically laminar as shown by the schlieren pictures (lambda shock). The recording of one of the flutter phenomena is reproduced below; Fig.32: highly explosive onset of flutter at an infinite Mach number of 0.922 with an oscillation frequency of 40 cps; Fig.33: end of flutter which is very little sinusoidal and somewhat precedes transition to the highly nonlinear amplitude domain corresponding to the aileron divergence, above Mach 0.96.

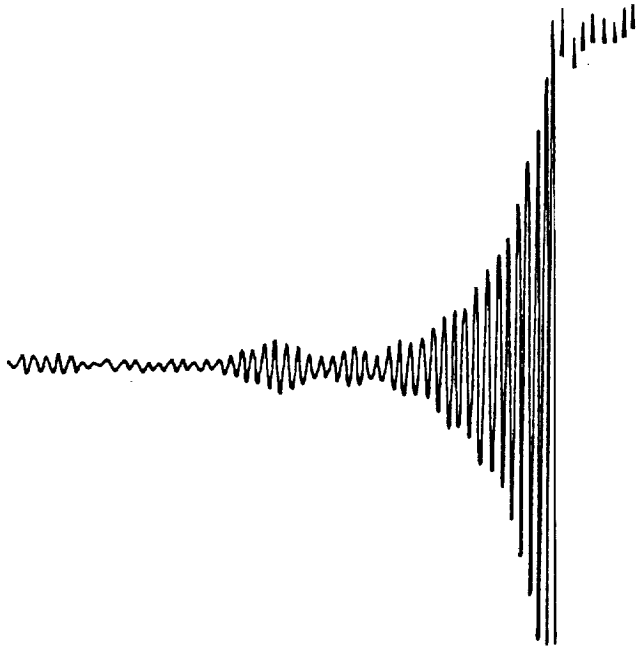

Fig.32

Supersonic flutter has not been systematically observed in laminar flow.

The pattern in Fig.33 shows the rapid variation in frequency on emergence from the instability range: in the zone A, f = 40 cps; in the zone B at a very similar Mach number (variation of about 0.01), f = 30 cps. /26

The 60 frames shown in Fig.34 correspond to a complete cycle during onset of flutter at an already high amplitude. Two vertical lines indicate the leading edge and the trailing edge of the aileron.

When the Mach number increases slowly, the recompression shock wave first recedes without oscillating. As soon as the wave reaches a certain position aft of the aileron hinge, the vibration is damped. Note that the recompression

takes place in two stages, which is well defined on the frames. The amplitude of motion of the downstream shock increases up to the point at which this shock periodically contacts the hinge. It seems that this constitutes a limiting amplitude for a given fixed Mach number. As soon as the Mach number continues to increase, the downstream shock moves away from the hinge; the amplitude of its motion increases in such a manner that the shock wave always reaches the same limit position constituted by the hinge. Finally, beyond a certain value of M, the amplitude decreases rapidly and the shock wave becomes stabilized.

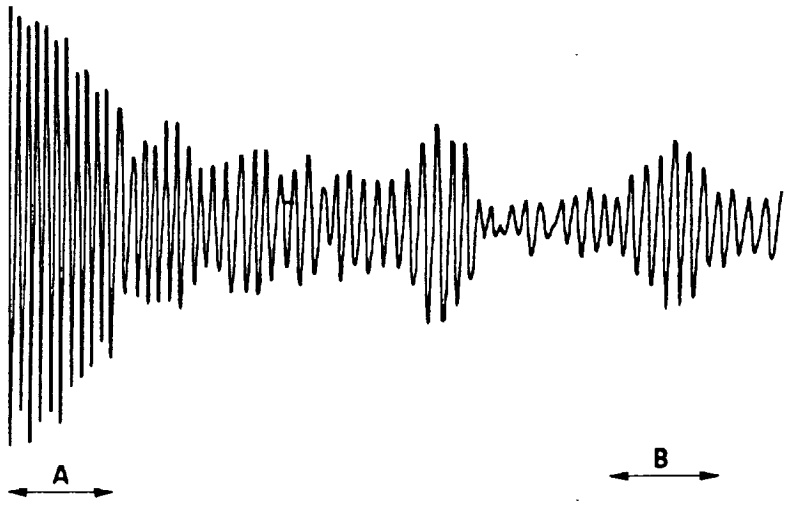

Fig.33

Denoting by $\frac{x}{c}$ the dimensionless abscissa of the base of the downstream shock with respect to the hinge, one obtains the curves in Fig.35 for the onset of flutter; in Fig.36 for the phase immediately before the aileron reaches the stops; in Fig.38 for the instant at which the amplitudes are limited by the stops; in Fig.39 for the instant of termination of flutter.

The oscillation amplitude of the aileron is practically proportional to that of the shock wave at fixed Mach number (Fig.35).

This proportionality coefficient $\left\{\frac{\text{aileron amplitude}}{\text{shock wave amplitude}}\right\}$ increases /27 with the Mach number (Figs.35 and 39).

At low amplitudes, the motions of the downstream shock and of the aileron are sinusoidal (Fig.35). When the amplitude increases, the motion of the aileron will remain sinusoidal but that of the shock wave will differ from sinusoidal as soon as the shock approaches the hinge. The motion will return to sinusoidal when the shock wave oscillates sufficiently far from the hinge (Fig.39) even if the motion of the aileron is no longer sinusoidal (effect of the stops: specifically Fig.39).

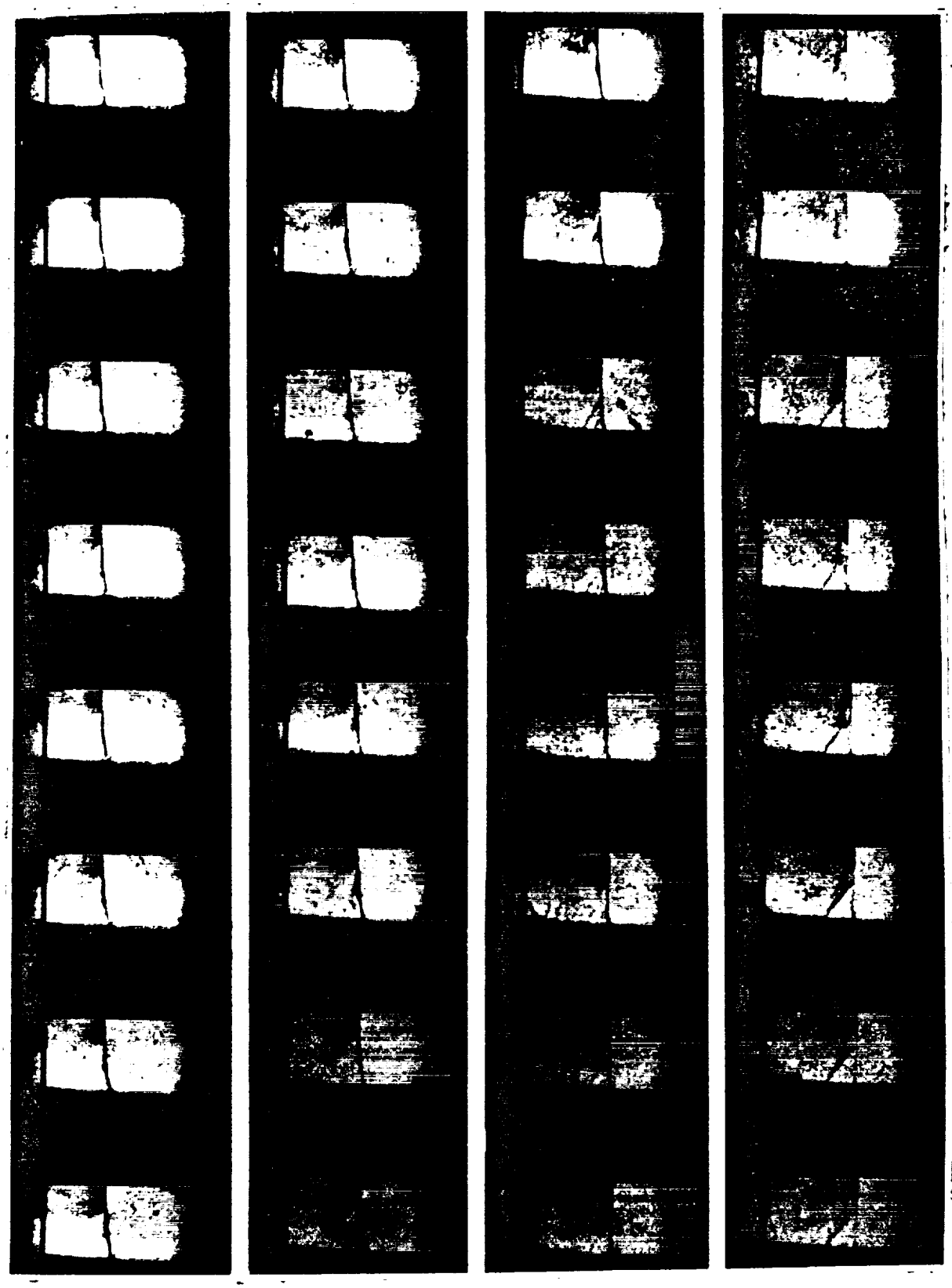

Fig.34

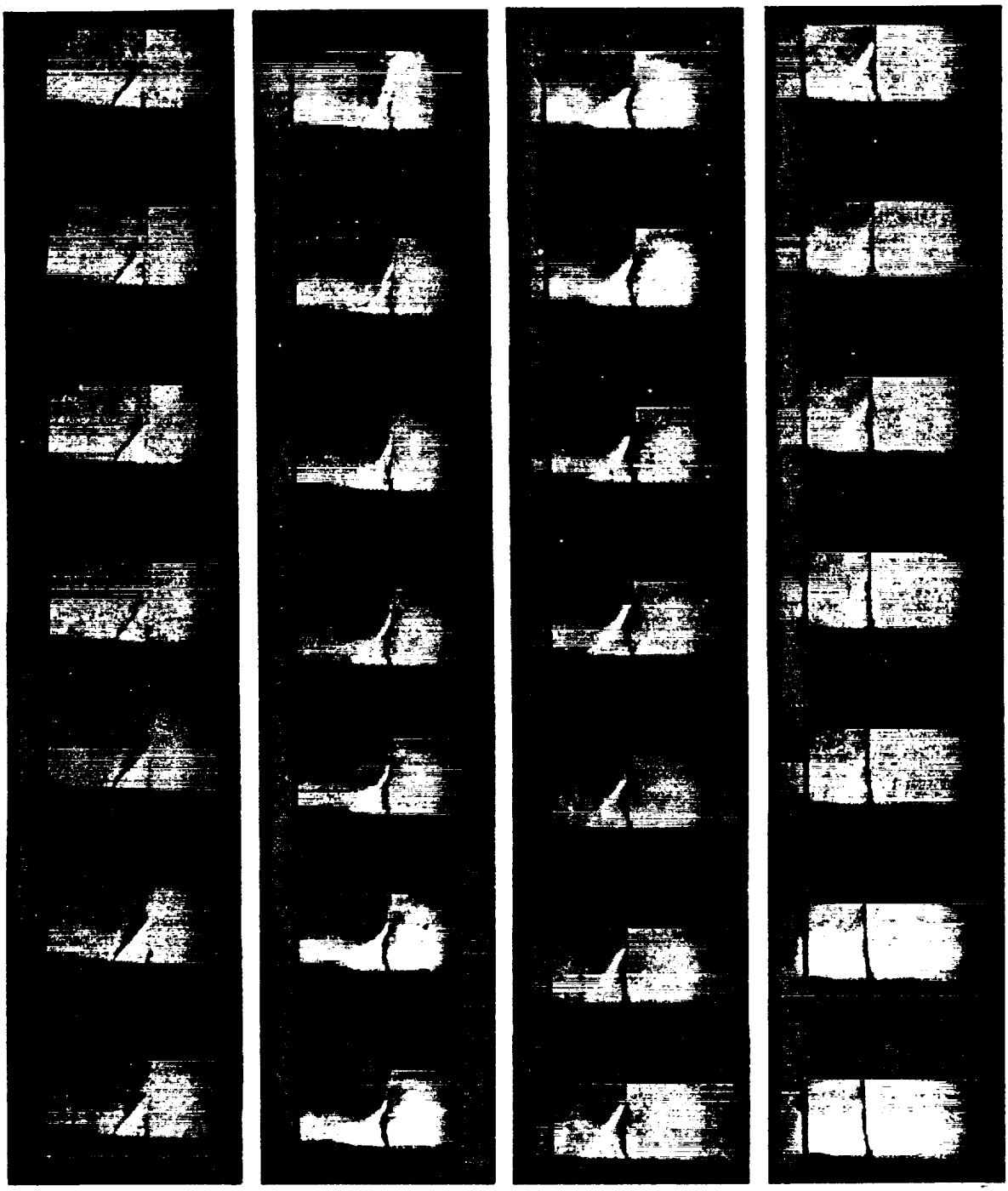

Fig.34 (cont'd) $\tau = 0.3$ - Laminar Flow.

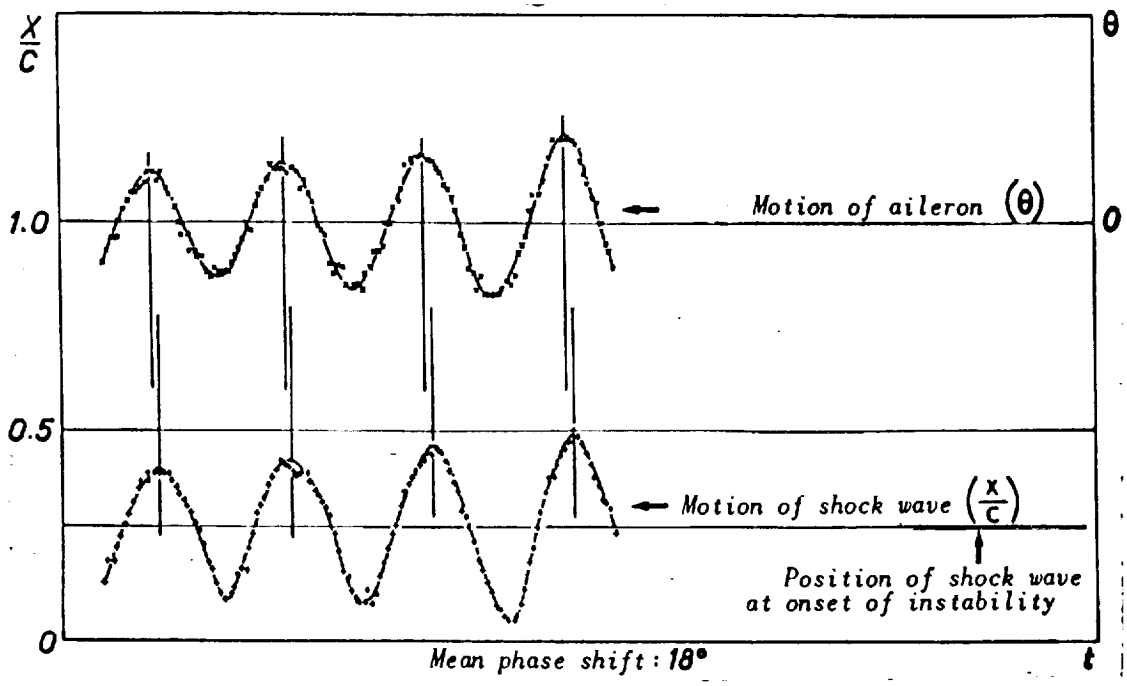

Fig.35 Aileron τ = 0.3 - Laminar Flow - Onset of Flutter.

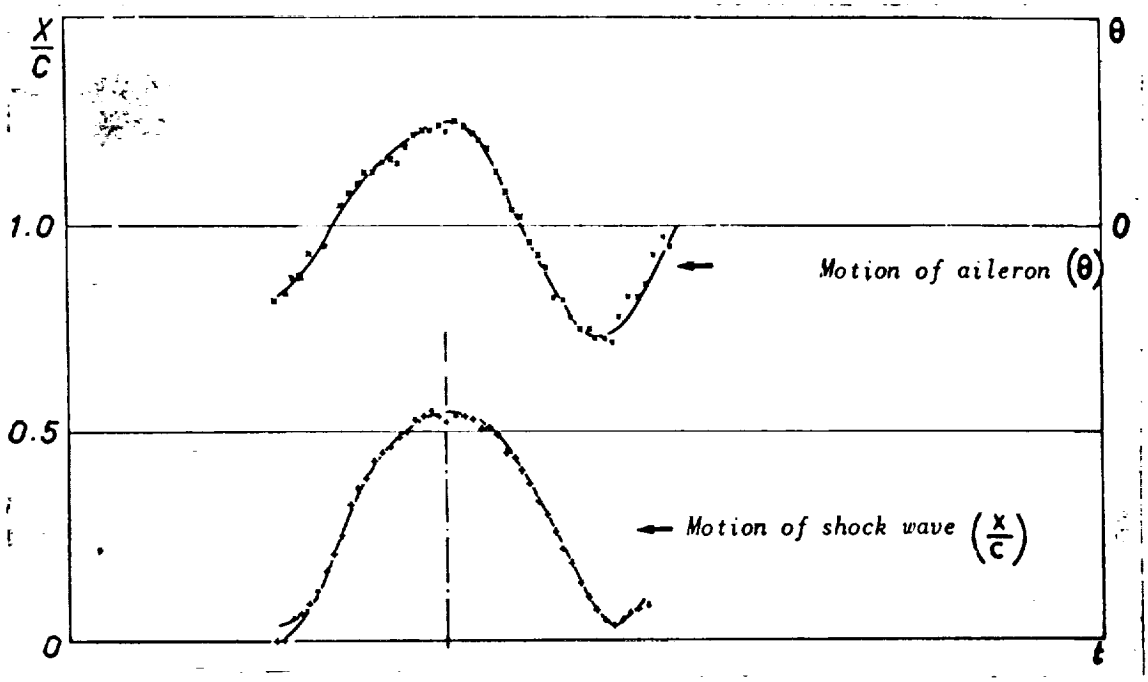

Fig.36 Aileron τ = 0.3 - Laminar Flow - Flutter.

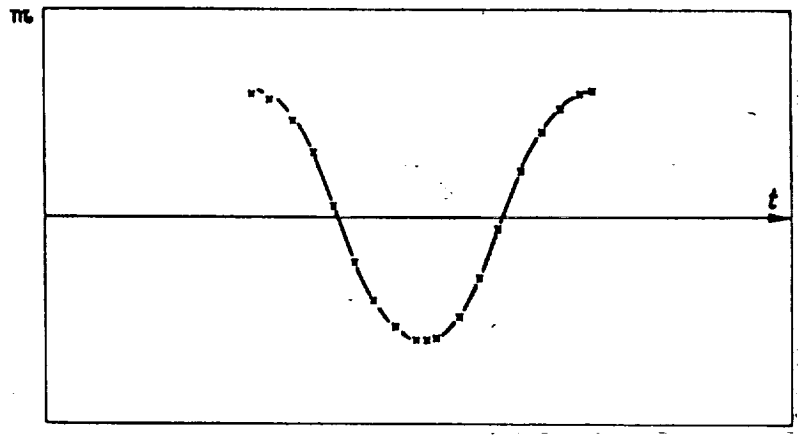

Fig.37

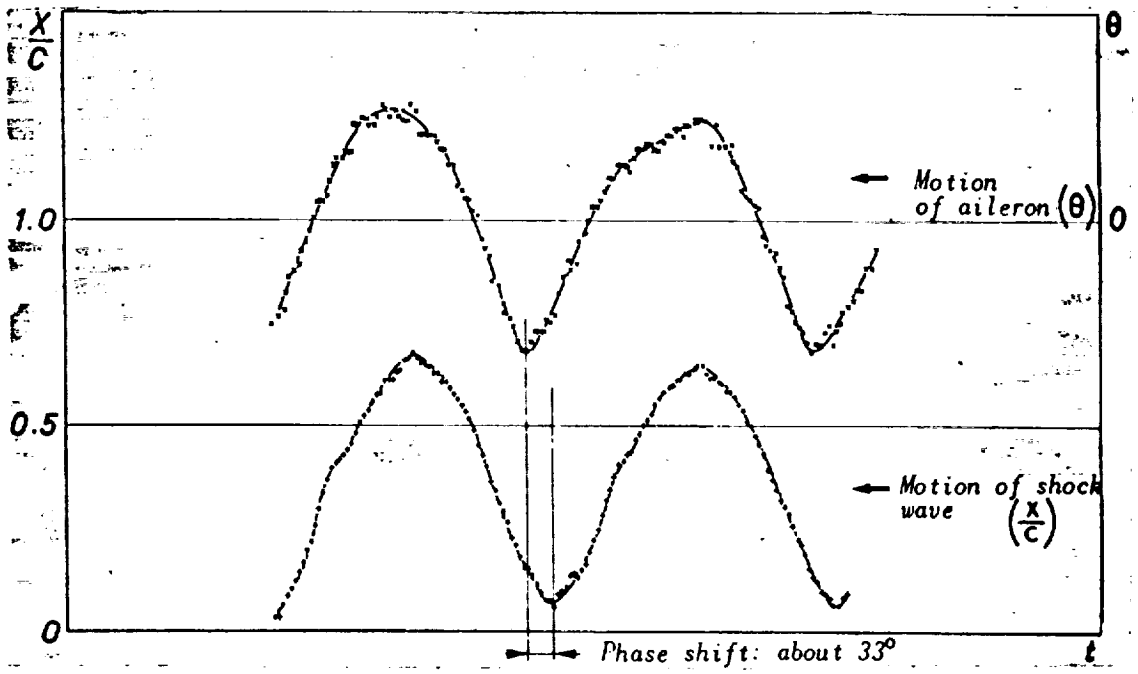

Fig.38 Aileron $\tau = 0.3$ - Laminar Flow - Flutter Stabilized by Stops.

It is of interest to study the variation in the aerodynamic hinge moment due to different positions of the shock waves on the pressure and suction sides, using the curve in Fig.36 as a typical example, as a function of the position /31 of the observed shock wave.

For this, it is assumed that the pressures upstream of the shock wave on the suction and pressure sides are identical and constant during the motion of the shock wave, at least at the level of the aileron. Let us denote this by p_M. We will make the same hypothesis with respect to the pressures downstream of the

shock waves, with p_v being the corresponding value. Locally, this will lead to rather large errors, but from the overall viewpoint the hypothesis is nevertheless justified (Fig.40).

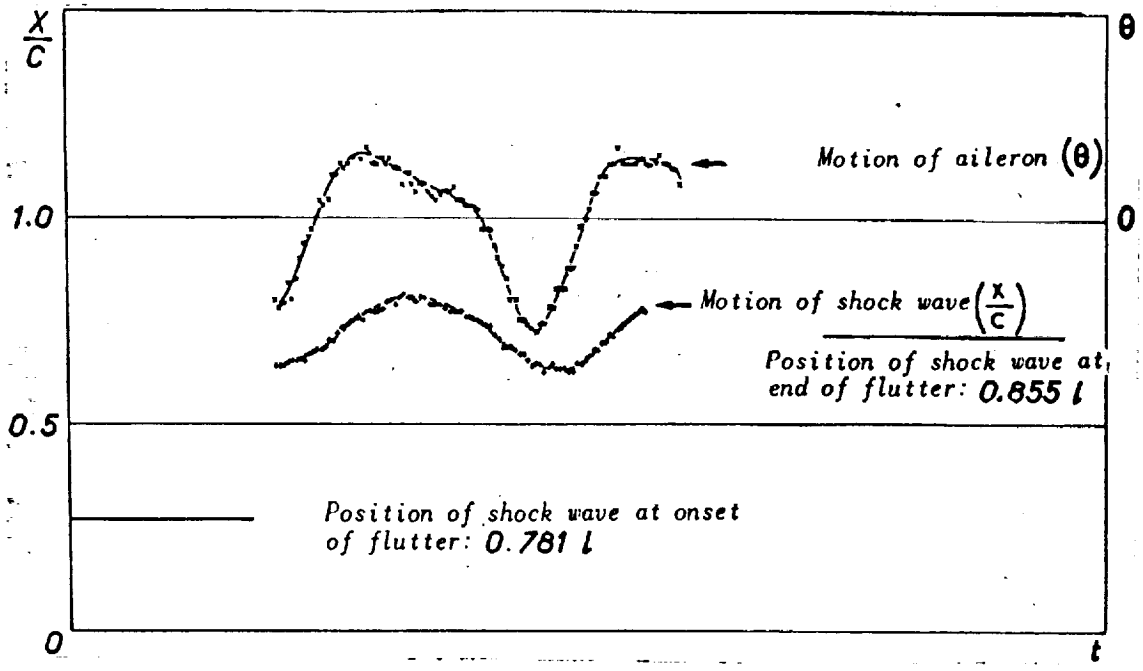

Fig.39 Aileron $\tau = 0.3$ - Laminar Flow - End of Flutter.

Thus, the hinge moment due to the shock wave will be

$$(p_v - p_M)(x_i - x_e)\frac{x_i + x_e}{2} = \mathfrak{M} \quad \text{with} \quad \mathfrak{M} = A(x_i^2 - x_e^2).$$

If it is assumed that the curve in Fig.36 gives x_e, then the curve x_i will be the same but out of phase by a half-period. For the hinge moment, the curve in Fig.37 is then obtained, which is very close to sinusoidal. /32

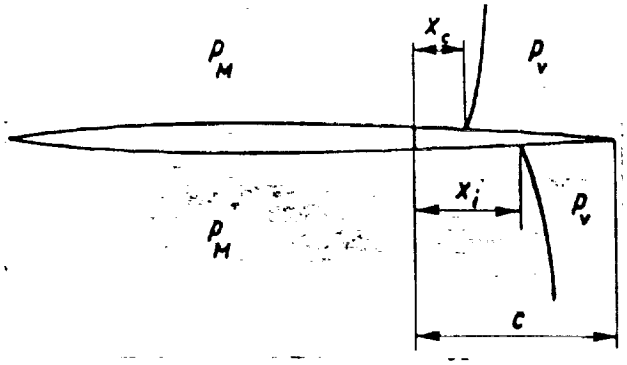

Fig.40

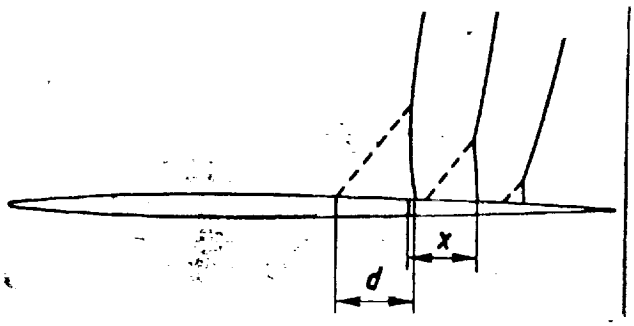

Fig.41

The lambda configuration of the shock wave evolves during the motion, as indicated in Fig.41.

The deviation d, at the level of the profile between the two recompression shocks, reaches a maximum value as soon as the wave is in the upstream position; it tends to zero in the downstream position.

Figure 34 distinctly shows the first shock wave when it is in the upstream position. This wave becomes less visible as it shifts toward the rear since it then becomes superposed to the expansion waves emerging from the aileron hinge. On projection of the film, this is clearly observable over the entire duration of the cycle.

Let us consider Fig.42.

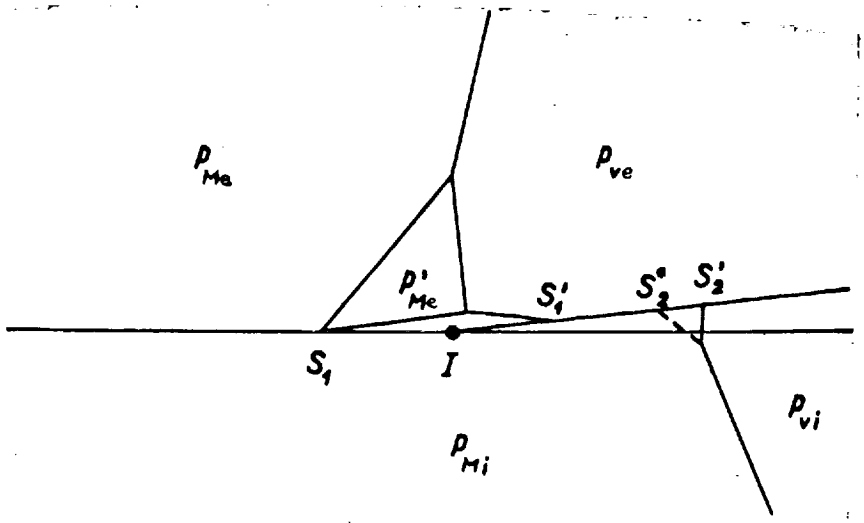

Fig.42

Let us assume that the aileron is shifted from its equilibrium position, /33 as indicated in the diagram.

On the suction side, the shock wave is in the bow position with a first recompression shock quite upstream of the second wave. In the schlieren picture, a separation of the boundary layer at the point S_1 can be observed.

On the pressure side, the shock wave is in the rear position, with an almost zero separation zone. The pressures in the various regions are p_{Me}, p'_{Me}, p_{Mi}, p_{ve}, p_{vi}. Since p_{Mi} is superior to p_{ve}, a rather intense restoring moment due to the shock waves exists which is superposed to the moment of aerodynamic forces without shock, and the aileron has the tendency to return to its equilibrium position at zero incidence which results in a dual effect:

The downstream shock wave at the suction side recedes.
The flow of the fluid in the opposite direction in the flow separation zone is less intense, since the pressure difference between p_{ve} and p'_{Me}

diminishes. Consequently, the length d between the upstream and downstream shock waves decreases. This is what one actually observes.

A certain lag exists between the motion of the aileron and the resultant motions of the shock waves.

On the pressure side, exactly the opposite takes place: p_{v_i} increases, the shock wave advances, the inverse flow increases, and the separation zone enlarges with a phase shift toward the rear relative to the aileron oscillation. This reasoning supposes that one is far below the oscillation frequency of the shock waves, considered as a system of one degree of freedom. This is actually the case when referring to the experimentally obtained values for a fixed airfoil (Ref.1).

For the phase shift calculations made by Coupry the reader is referred to his paper (Ref.5). In reality, the hinge moment is not due exclusively to the presence of shock waves so that the flutter is definitely attenuated when considering the other aerodynamic forces.

The magnitude of damping due to the shock waves can be calculated from steady-state conditions experimentally established for the same airfoil with locked aileron and measured as a function of the boundary layer thickness so as to allow for the Reynolds number.

V.2.2 Turbulent Flow

a) Transition at the Wing Leading Edge

Instability still exists, although damped, as shown by the recordings of onset (Fig.43) and end of flutter (Fig.44). /34

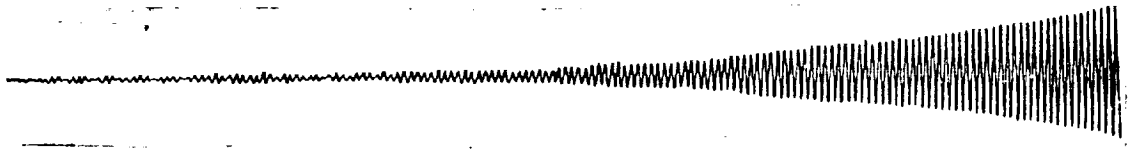

Fig.43 Aileron $\tau = 0.3$ - Transition Induced at the Leading Edge. Initial frequency without wind: 75 cps; frequency of flutter onset: 82.5; frequency of flutter end: 81.3 (instability of type B).

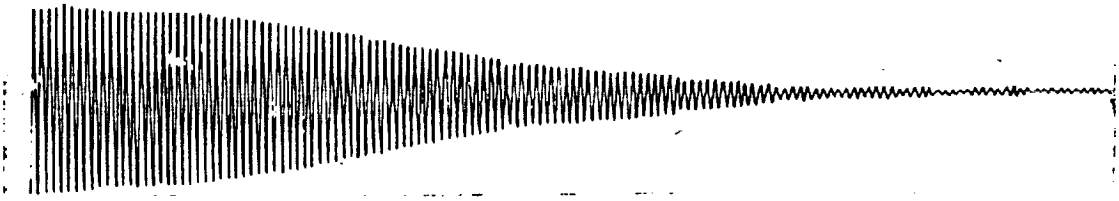

Fig.44 End of Flutter (Continuation of Fig.43).

The end of flutter is followed by divergence and then by the instability C starting from Mach 1.07, which is produced more spontaneously in a turbulent flow.

b) Transition Induced at Leading Edge and Main Bulkhead

Here, the instability disappears completely. If the aileron is excited in its phase resonance and if the excitation is then stopped, the aileron will damp as indicated on the recordings (Figs.45a, b, c).

On increasing the Mach number from 0.90 to 1.0, without excitation of the aileron, a slight vibration of the aileron will appear which is rather random and not very sinusoidal close to 0.94 (Fig.46).

135

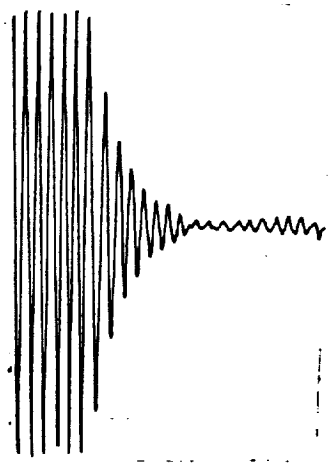

Fig.45a Excitation of an Aileron of 0.3 Relative Chord, Followed by Relaxation in Transition Induced at the Main Bulkhead at M = 0.897. The initial frequency without wind was 18 cps; the frequency during relaxation was 26 cps.

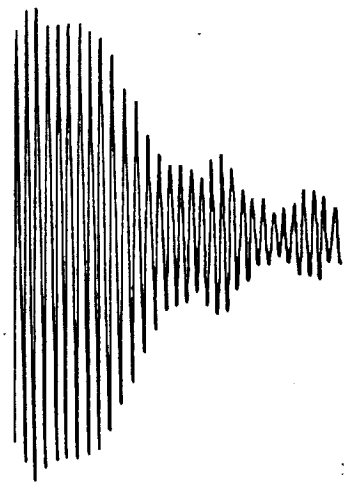

Fig.45b Relaxation at M = 0.922; Frequency, 32.5 cps.

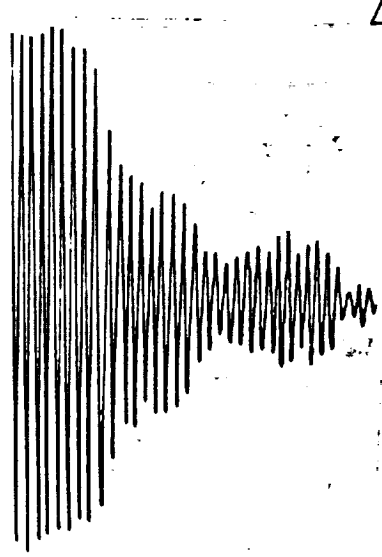

Fig.45c Relaxation at M = 0.940; Frequency, 33.0 cps.

Fig.46 M = 0.94, Approximately.

The damping reaches a minimum at 0.94 but is still above the damping without wind.

The three photographs (Figs.47a, b, c) show three phases of the flow.

a)

b)

c)

Fig.47 Aileron of Relative Chord $\tau = 0.3$ - Transition Induced at Leading Edge and Main Bulkhead.
a - Recompression shock on the aileron hinge; b - Recompression shock at the center of the aileron chord (no instability);
c - Recompression shock at the trailing edge.

V.3 Observations on an Aileron with 0.5 Relative Chord

V.3.1 Laminar Flow

No quantitative experiments were made on laminar flow.

V.3.2 Turbulent Flow

a) Transition at the Leading Edge

The observed flutter is relatively little explosive compared to that observed in laminar flow (Figs.48a and b).

In the supersonic regime, a low explosive flutter of type C appears, which stabilizes at moderate amplitudes.

/37

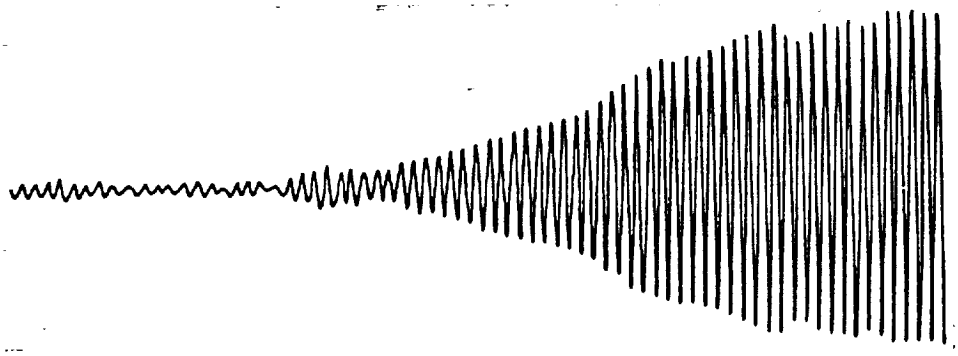

Fig.48a Aileron of 0.5 Relative Chord; Transition Initiated at the Leading Edge; Flutter of Type B. Initial frequency without wind: 32.5 cps; frequency of flutter onset: 53.5 cps.

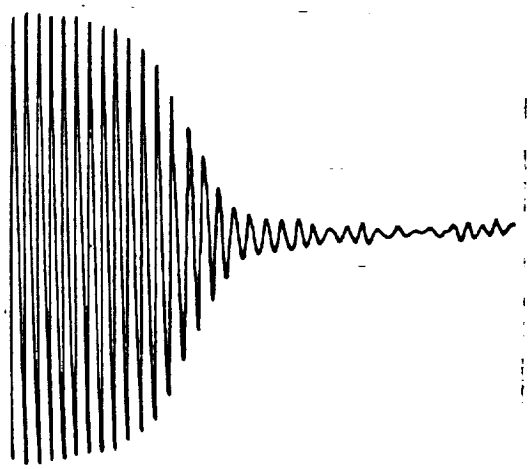

Fig.48b End of Flutter f = 45 cps.

Fig.49

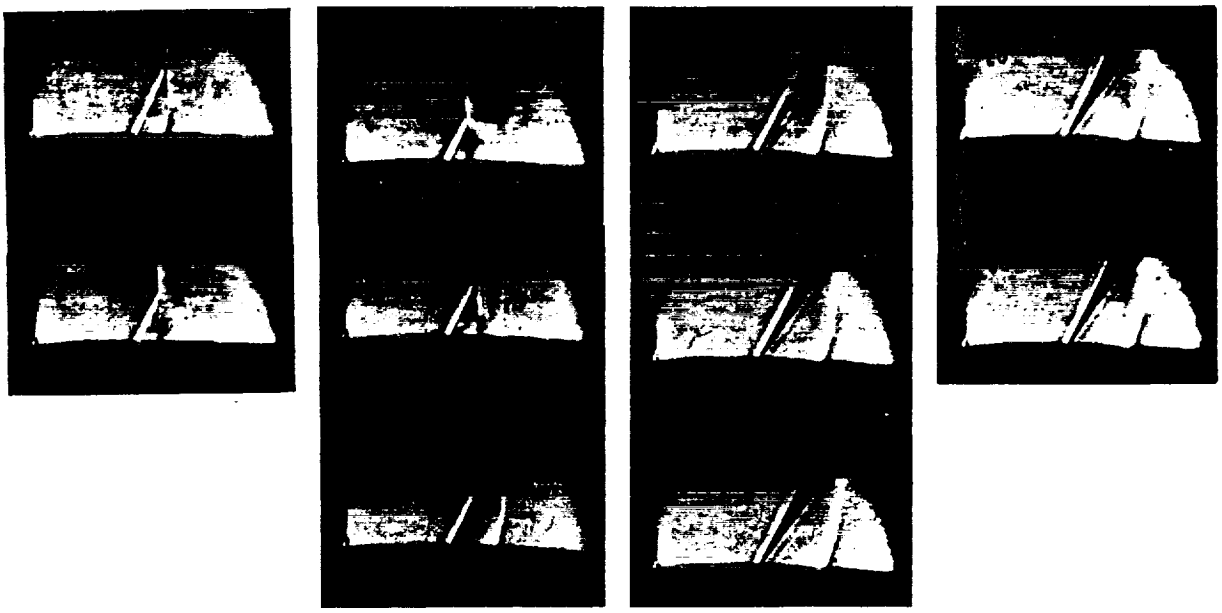

Fig.49 (cont'd) Aileron $\tau = 0.5$ - Transition Initiated at the Leading Edge - Flutter of Type B (during Increase in Amplitude).

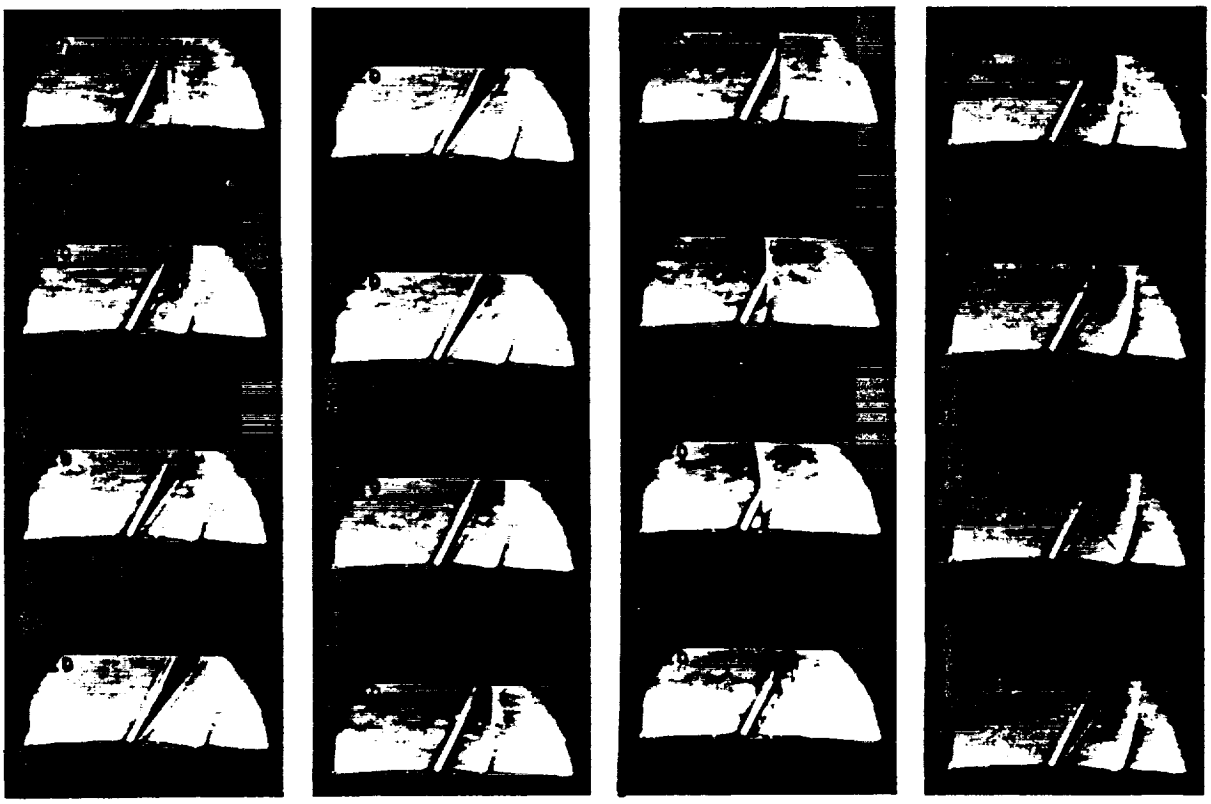

Fig.50

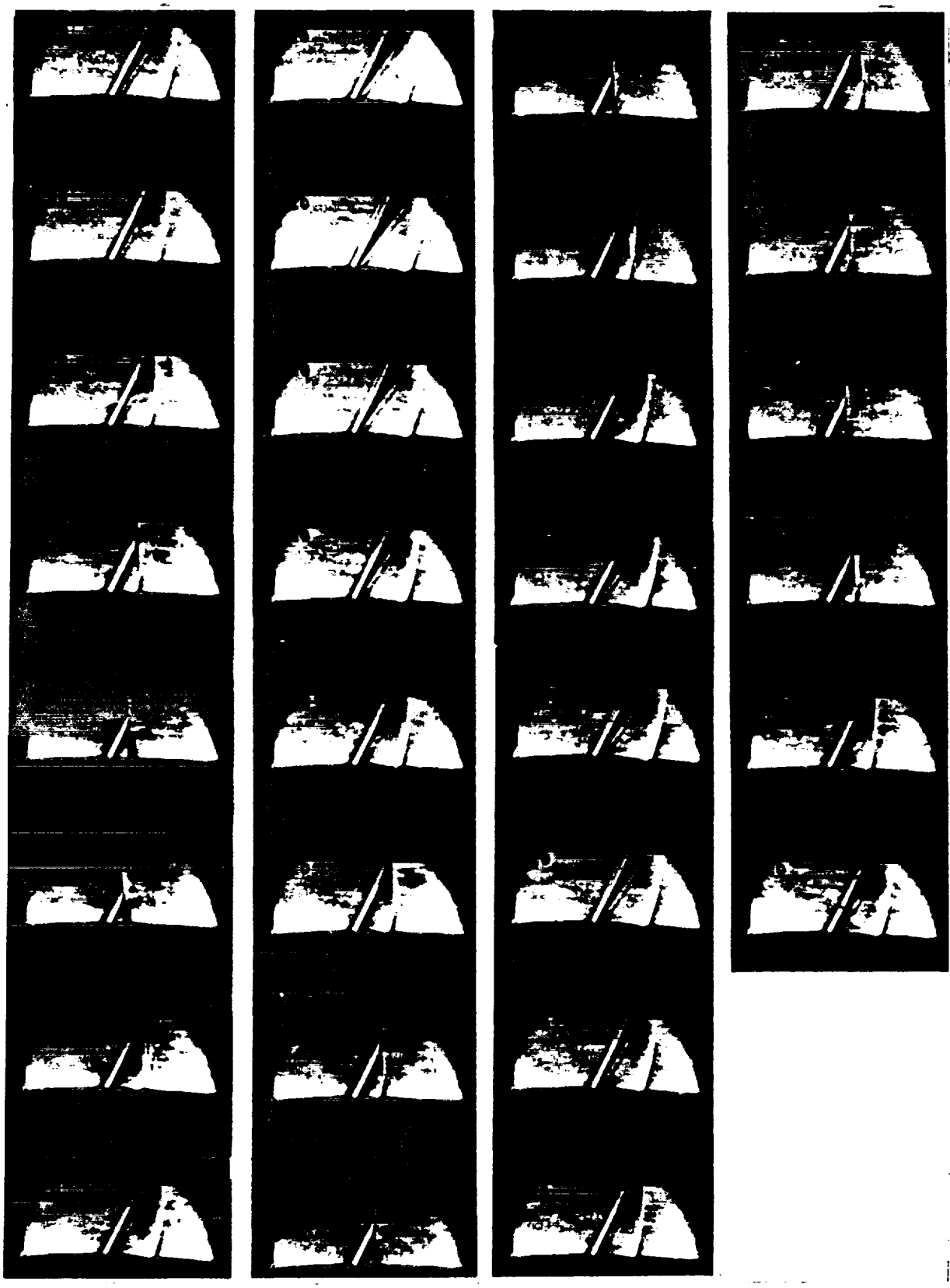

/40

Fig.50 (cont'd) Aileron τ = 0.5 - Transition Initiated at the Leading Edge - Flutter of Type B.

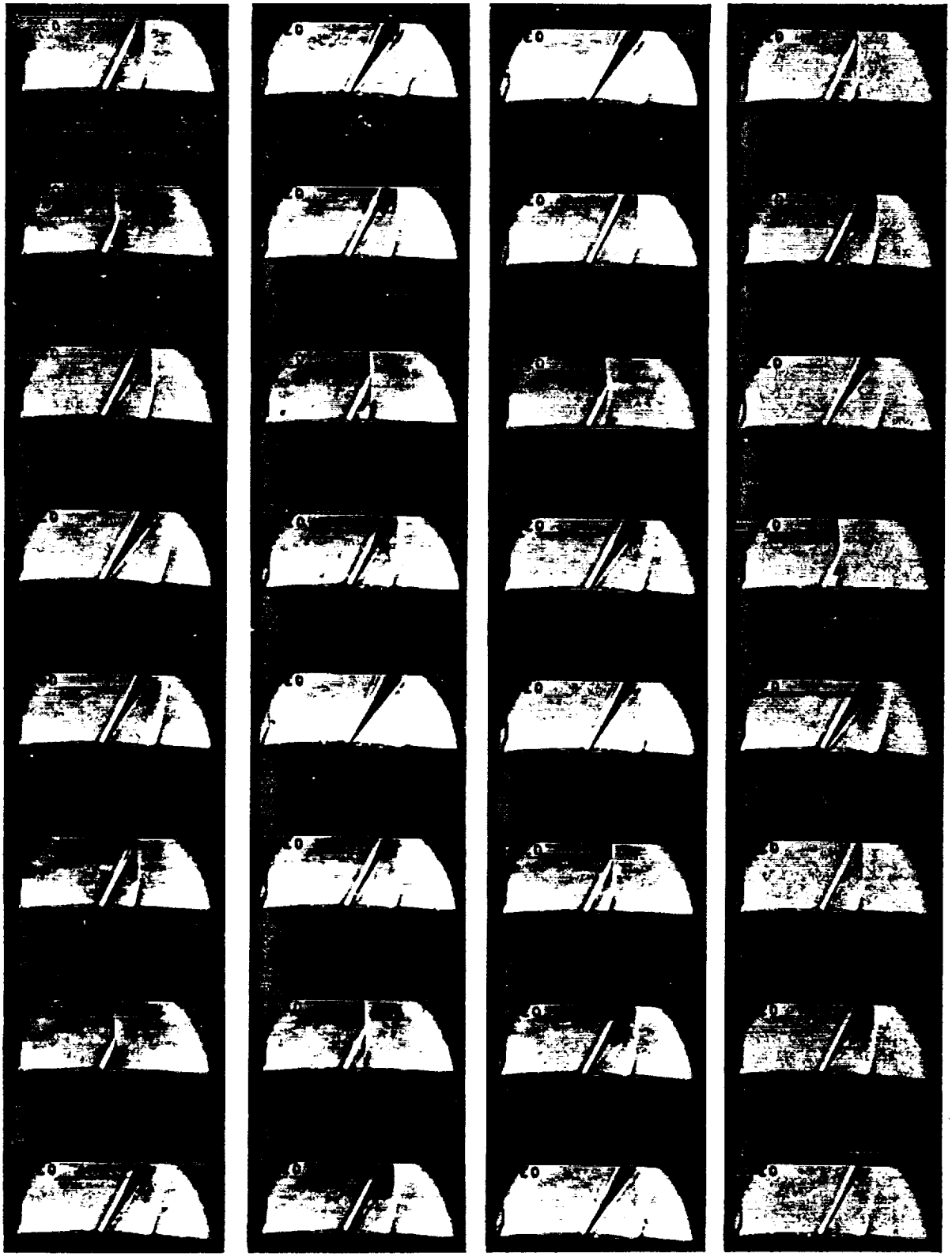

Fig.51 Aileron $\tau = 0.5$ - Transition Initiated at the Leading Edge - Flutter of Type B Stabilized by the Stops.

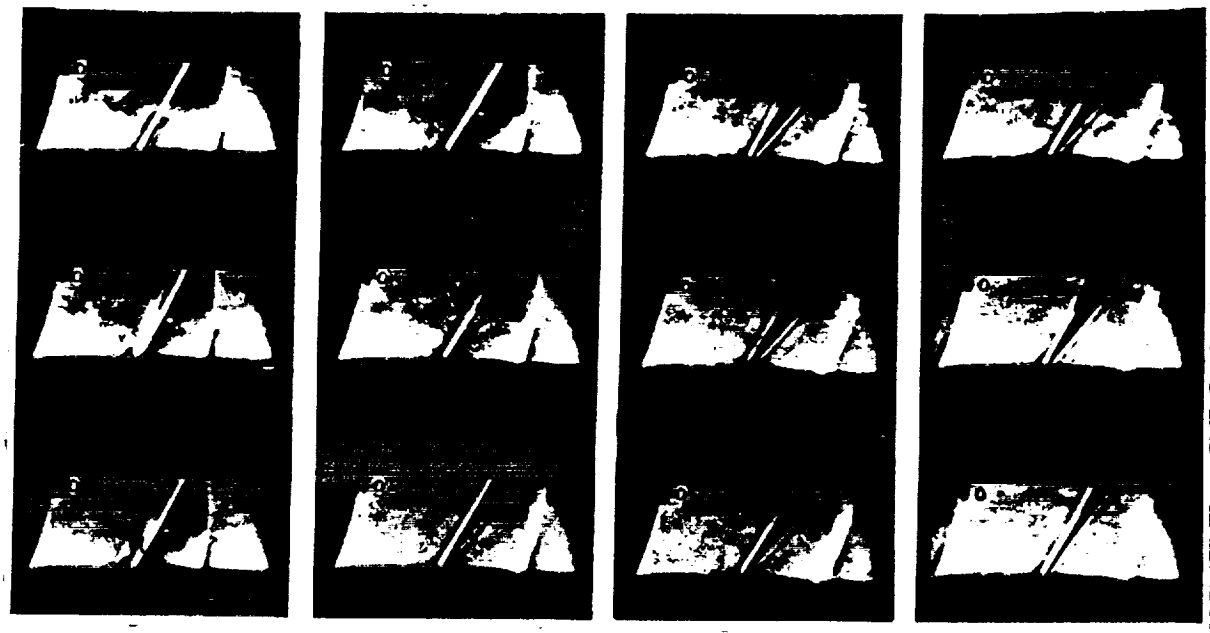

/42

Fig.52 End of the Instability B.

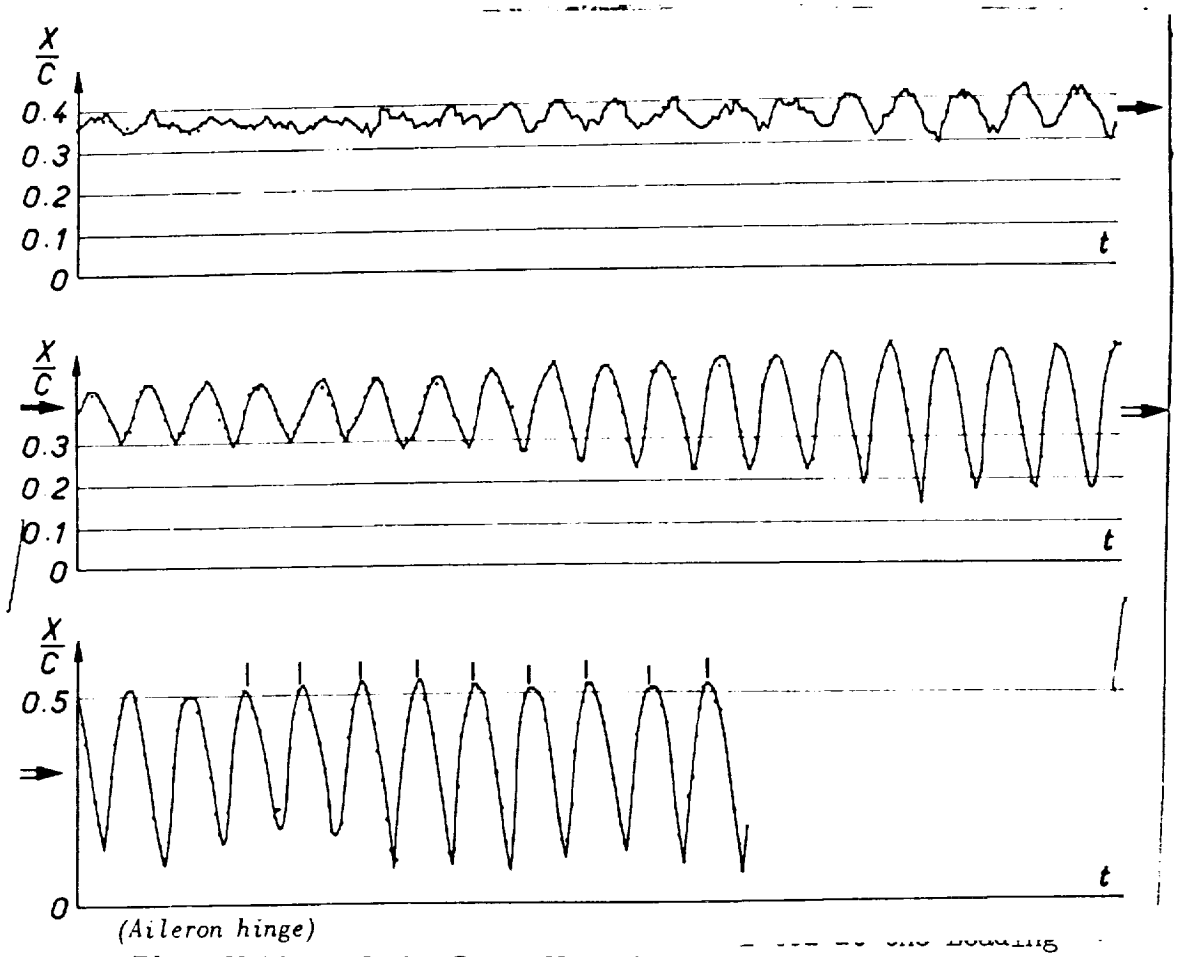

Edge; Motion of the Shock Wave during Onset of Flutter (Compare with the Recording in Fig.47).

Schlieren Pictures:

The photographs in Figs.49, 50, 51, and 52 show the motion of the shock waves at various stages of flutter.

Figure 53 shows the position of the shock wave as a function of time. Here, we have no corresponding motion of the aileron except the times corresponding to passage through the maximum positions and represented by vertical reference lines for the last cycles of the recording strip.

Figure 54 corresponds to the phase of increasing instability shortly before the aileron touches the stops (the time scale has been enlarged). The arrows indicate passage of the aileron through the maximum and minimum positions. The slope is not sinusoidal (see the case of an aileron of 0.3 relative chord).

At the end of flutter, the motion of the shock wave is weak while that of the aileron remains very strong. The end of flutter sets in rapidly.

The shock wave here is simple and no separation of the boundary layer can be detected.

Figure 55 gives schlieren pictures of the supersonic instability C.

b) Transition at the Leading Edge and Main Bulkhead

Here, the instability disappears as in the case for an airfoil with 0.3 relative chord.

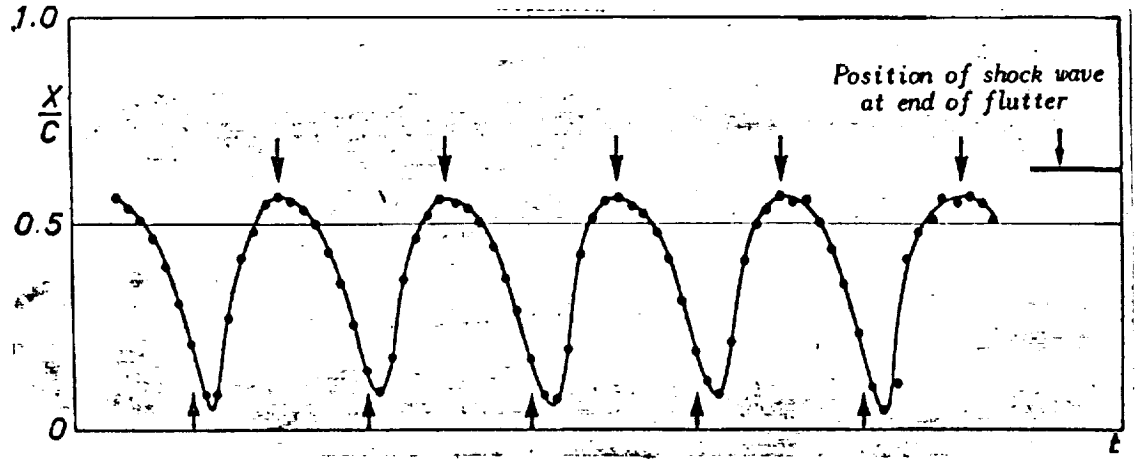

/43

Fig.54 Aileron $\tau = 0.5$ - Transition Initiated at the Leading Edge; Motion of the Shock Wave before Reaching Maximum Amplitude.
The arrows indicate the times corresponding to the amplitude maximum and minimum of the aileron.

V.4 Flutter Domains

In laminar flow, for an aileron of 0.3 relative chord, the shock wave at the onset of flutter is at 78% of the total chord of the wing while, at the end of the instability, it is at 91.3%.

In the case of flow transition initiated at the leading edge, the instability zone is more narrow.

For an aileron of 0.5 relative chord, with transition at the leading edge, the positions of onset and end of flutter are 68 and 81.5%, respectively.

VI. CONCLUSIONS

The totality of these tests permits clarifying or confirming certain aspects of single degree of freedom instabilities in the transonic regime.

Flutter with the shock wave upstream of the aileron hinge has never been observed. This may be due to the following circumstances:

Negligible relative thickness of the profile.
High values of the relative chords of the tested ailerons (1.0; 0.5; 0.3). For $\tau = 0.5$, only the instability B can exist since the shock wave appears very close to the hinge. For $\tau = 0.3$, the Mach number range, comprised between the critical Mach number of the profile and the value for which the shock reaches the aileron, is relatively narrow. If flutter exists at all, it must be encountered for ailerons of low relative chord (for example, tabs).

The instabilities of type B are always observed in two-dimensional cases /45 when the thickness of the turbulent boundary layer is small. The Mach number of flutter onset decreases with increasing chord of the aileron. The Mach number of flutter end is not very sensitive to the value of the chord. Thus, it is probable that no flutter exists on the tabs, in contradiction to the preceding type (A).

The flutter B is highly sensitive to two influences:

Reynolds number; the Mach numbers of onset and end of the instabilities increase and decrease respectively, as soon as Re increases. The shock of lambda form is no longer an essential characteristic.
Aspect ratio; the flutter disappears rapidly as soon as the aspect ratio decreases.

(The effect of reduced frequency was not studied at high values.)

The instability C is very little sensitive to the effects of aspect ratio and Reynolds number (study limited to low frequencies). This instability exists for all types of wings: two-dimensional wing, straight wing of low aspect ratio, delta wing, no matter what the position in the aileron plane might be. The

/44

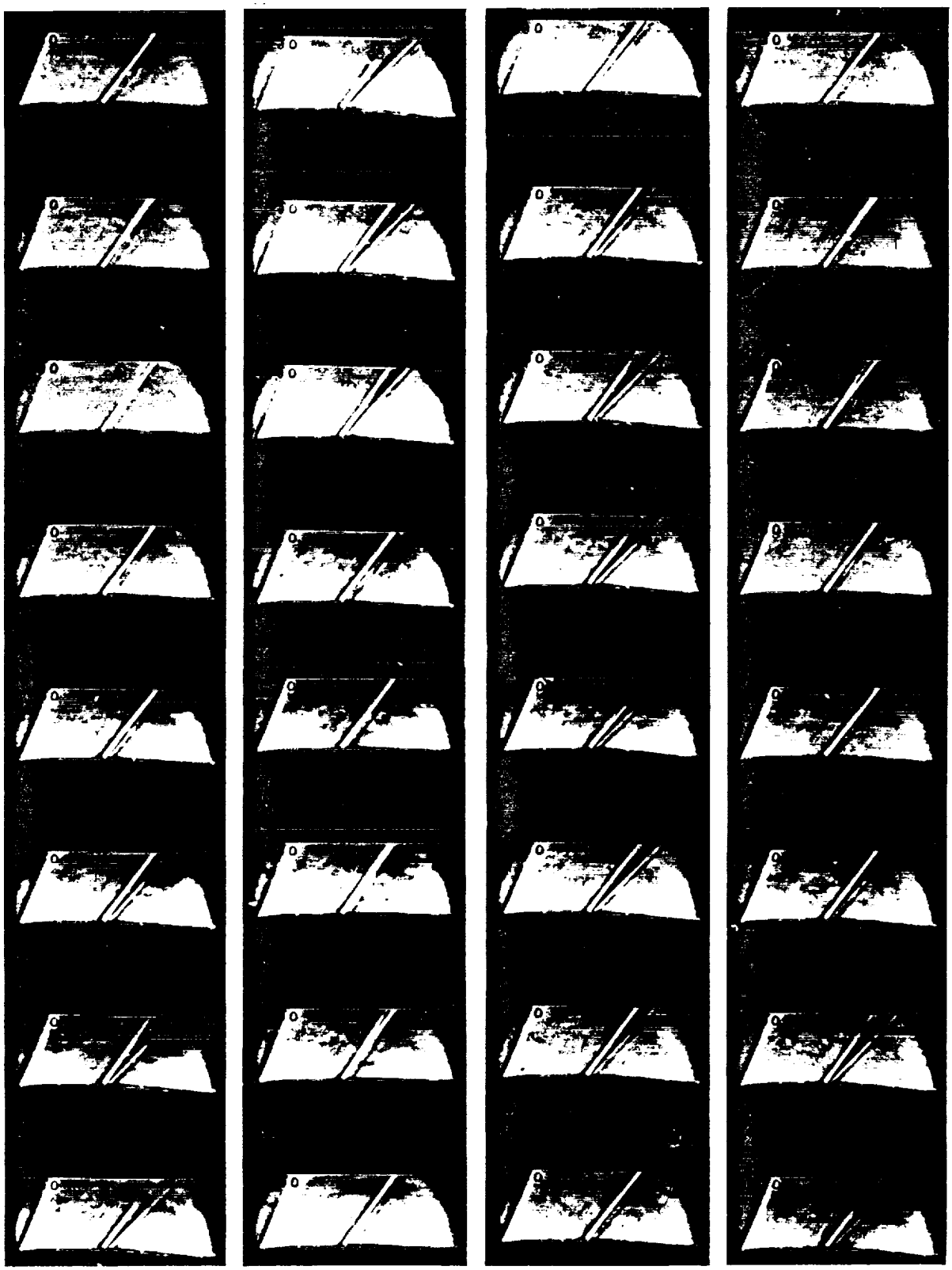

Fig. 55

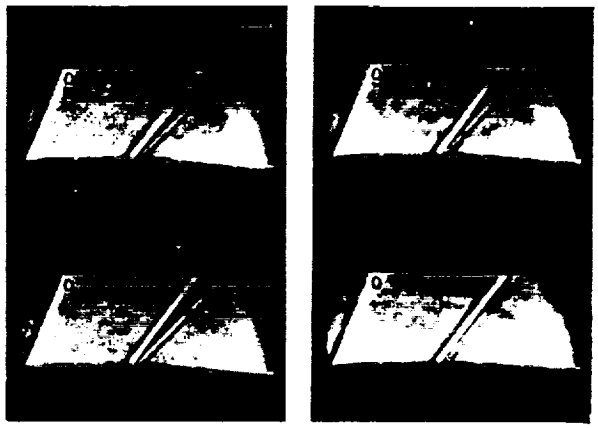

Fig.55 (cont'd) Aileron $\tau = 0.5$ - Transition Initiated at the Leading Edge; Supersonic Flutter (Type C)

flutter is not very explosive and stabilizes at relatively low amplitudes. Flutter is more distinct in turbulent flow.

Finally, the three instability domains (in the presence of flutter of type A) are very distinct. The first two domains are clearly separated by the stability zone which exists when the shock wave is attached to the hinge; the instability B and the instability C are separated by a zone about Mach 1.0, characterized by negative values of the real hinge moment coefficient and by very high positive values of the imaginary coefficient.

REFERENCES /46

1. Kawamura, R. and Karashima, K.: Instability of Shock Wave on Thin Airfoil in High Subsonic Flow. Proc. of the Seminar on Aeronautical Sciences, Bangalore, Vol.1.
2. Nakamura, Y. and Tanabe, Y.: Some Experiments on Control-Surface Buzz. Tech. Rept. of National Aerospace Laboratory, TR 721, Tokyo, 1964.
3. Lambourne, N.C.: Flutter in One Degree of Freedom. Manual of Aeroelasticity, AGARD, Vol.5, Part 5, Chapt.5.
4. Rebuffet, P.: Experimental Aerodynamics (Aérodynamique expérimentale). Supplement to the Second Edition, Librairie Béranger, Paris, 1965.
5. Coupry, G. and Piazzoli, G.: Study of Flutter in Transonic Regime (Étude du flottement en régime transsonique). Rech. Aeron., No.63, 1958.
6. Loiseau, H.: Measurements of Nonstationary Aerodynamic Coefficients of Control Surfaces in the Transonic Regime (Mesures de coefficients aérodynamiques instationnaires de gouvernes en transsonique). Rech. Aeron., No.97, 1963.
7. Loiseau, H.: Measurements of Coefficients for Wings of Low Aspect Ratio in Transonic Regime (Mesures de coefficients d'aileron de faible allongement en transsonique). ONERA, Tech. Note No.75, 1964.
8. Tables of Aerodynamics Coefficients for an Oscillating Wing-Flap System in a Subsonic Compressible Flow. Rept. F.151, National Luchtvaartlaboratorium, Amsterdam, May 1954.

Translated for the National Aeronautics and Space Administration by the O.W.Leibiger Research Laboratories, Inc.